Geological Survey of Canada
Open File 4822

KIMBERLITE INDICATOR MINERAL CHEMISTRY AND TILL GEOCHEMISTRY AROUND THE SEED AND TRIPLE B KIMBERLITES, LAKE TIMISKAMING, ONTARIO

M. B. McClenaghan, I. M. Kjarsgaard, and B. A. Kjarsgaard

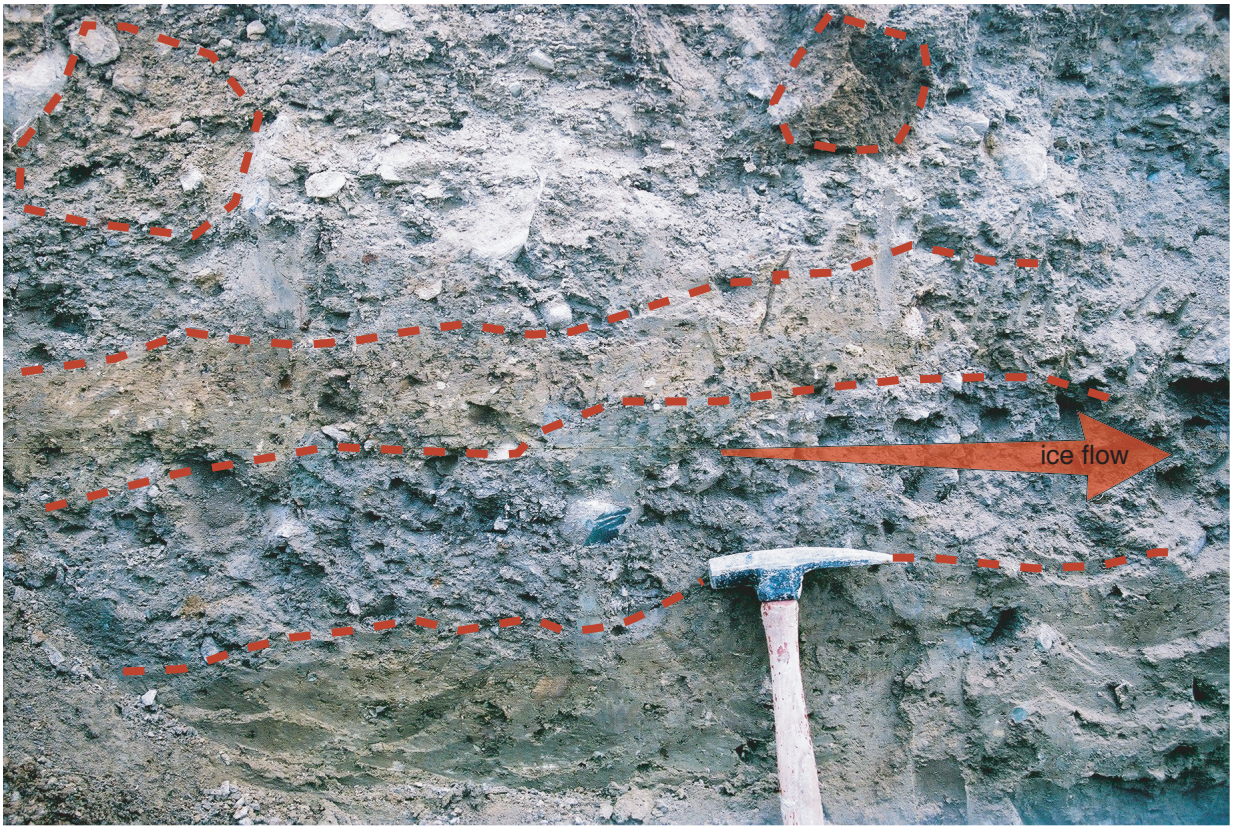

2004

Natural Resources Canada
Ressources naturelles Canada
Canada

Geological Survey of Canada
Open File 4822

KIMBERLITE INDICATOR MINERAL CHEMISTRY AND TILL GEOCHEMISTRY AROUND THE SEED AND TRIPLE B KIMBERLITES, LAKE TIMISKAMING, ONTARIO

M. B. McClenaghan[1], I. M. Kjarsgaard[2], and B. A. Kjarsgaard[1]

1. **Geological Survey of Canada, 601 Booth Street, Ottawa, Ontario K1A 0E8**
2. **Consulting Mineralogist, 15 Scotia Place, Ottawa, Ontario, K1S 0W2**

McClenaghan, M.B., Kjarsgaard, I.M., and Kjarsgaard, B.A.
2004: Kimberlite Indicator Mineral Chemistry and Till Geochemistry around the Seed and Triple B Kimberlites, Lake Timiskaming, Ontario; Geological Survey of Canada, Open File 4822, 27 p., 1 CD-ROM.

Open files are products that have not gone through the GSC formal publication process.

Cover illustration:
Orange-brown bands of kimberlite-rich till (outlined with red dashed lines) and grey argillite-rich (local country rock) till overlying the southern part of the Triple B kimberlite.

©Her Majesty the Queen in Right of Canada 2004
Available from:
Geological Survey of Canada
601 Booth Street
Ottawa, Ontario K1A 0E8

TABLE OF CONTENTS

ABSTRACT 1

INTRODUCTION 1

LOCATION AND ACCESS 1

GEOLOGY 2
- Local Bedrock Geology 2
- Kimberlite Geology 2
- Quaternary Geology 4

METHODS 4
- Sample Collection and Preparation 4
- Kimberlite Indicator Mineral Identification 5
- Geochemical Analysis of Kimberlite and Till 5

KIMBERLITE INDICATOR MINERAL ABUNDANCE 6
- Seed Kimberlite 6
- Triple B Kimberlite 7

PYROPE AND MG-ILMENITE SURFACE TEXTURES 11

KIMBERLITE INDICATOR MINERAL CHEMISTRY 11
- Mg-Ilmenite 11
- Garnet 12
- Cr-Diopside 14
- Chromite 14
- Olivine 15
- Enstatite 16

PEBBLE LITHOLOGY 16

KIMBERLITE GEOCHEMISTRY 17

TILL GEOCHEMISTRY 18
- Till at Bedrock Interface 21
- Shallow Till 21
- Comparison to Indicator Mineral and Pebble Counts 22

DISCUSSION 22
- Seed Kimberlite 22
- Triple B Kimberlite 24
- Till Geochemistry 25

CONCLUSIONS 25

ACKNOWLEDGMENTS 26

REFERENCES 26

APPENDICES
- Appendix A. Sample Descriptions and Locations
- Appendix B. Pebble Lithology Data for the 0.8 to 5 cm Fraction of Till Samples
  - Appendix B.1 Data listing
  - Appendix B.2 Digital colour photos of each sample
- Appendix C. Electron microprobe data for kimberlite Indicator minerals

Appendix C.1 Mg-ilmenite and ilmenite
Appendix C.2 Garnet
Appendix C.3 Cr-diopside
Appendix C.4 Chromite
Appendix C.5 Olivine
Appendix C.6 Enstatite
Appendix C.7 Perovskite
Appendix D. Kimberlite Indicator Mineral Abundance Calculations
Appendix D.1 Number of indicator mineral grains: a) visually counted; b) number of grains probed; c) number of grains confirmed by microprobe analysis; d) visual counts corrected; e) corrected counts normalized to 10 kg
Appendix D.2 Number of indicator mineral grains: a) visually counted; b) counts confirmed by microprobe analysis; c) visual counts corrected; d) corrected counts plus counts confirmed (b +c); e) counts normalized to 10 kg
Appendix E. Till Geochemical Data for Kimberlite and Till
Appendix E.1 Geochemical data for the Seed and Triple B kimberlites
Appendix E.2 $LiBO_2$ fusion/ICP-ES data for four size fractions of till around the Triple B kimberlite
Appendix E.3 $LiBO_2$ fusion/ICP-MS data for four size fractions of till around the Triple B kimberlite
Appendix E.4 Aqua regia/ICP-MS data for four size fractions of till around the Triple B kimberlite

KIMBERLITE INDICATOR MINERAL CHEMISTRY AND TILL GEOCHEMISTRY AROUND THE SEED AND TRIPLE B KIMBERLITES, LAKE TIMISKAMING, ONTARIO

M. B. McClenaghan[1], I. M. Kjarsgaard[2], and B. A. Kjarsgaard[1]

1. Geological Survey of Canada, Natural Resources Canada, 601 Booth St., Ottawa, ON K1A 0E8
2. Consulting Mineralogist, 15 Scotia Place, Ottawa, Ontario, K1S 0W2

ABSTRACT

In 2001 and 2002, shallow trenches were excavated by the Geological Survey of Canada through till into the Seed and Triple B kimberlites, in the northeast part of Firstbrook Township, near Lake Timiskaming, Ontario. The purposes of studying these two kimberlites were to document their kimberlite mineralogy and the glacial dispersal patterns associated with them. This report documents the chemistry of indicator minerals in the kimberlites and in till down-ice, as well as till matrix geochemical patterns associated with the Triple B kimberlite. The Triple B kimberlite consists of several different phases: hypabyssal kimberlite, dark green volcaniclastic ('diatreme') kimberlite, and its highly altered light green equivalent. Mg-ilmenite compositions in all three phases are very similar and resemble those for the Seed kimberlite. The Seed and Triple B kimberlites are two of four strong negative magnetic anomalies 240 m apart that define a 700 m northwest trend. Both kimberlites contain 1000s of indicator minerals in a 10 kg sample, the Seed kimberlite is dominated by Mg-ilmenite and the Triple B kimberlite is dominated by Mg-ilmenite, Cr-diopside and pyrope. The relative proportions of indicator mineral species are different from other kimberlites in the Lake Timiskaming kimberlite field and can be used to distinguish the Seed and Triple B dispersal trains from those derived from other nearby kimberlites.

Down-ice of the Triple B kimberlite, till contains predominantly kimberlite debris, giving it a green colour. The presence of abundant kimberlite pebbles and thousands of kimberlite indicator minerals results in elevated concentrations of MgO, Ni, Ba, LREE, Ta, Nb, TiO_2, P_2O_5, Cr_2O_3, Sr, Th, U, and CaO in the till. These elements are most enriched in the <0.063 mm (silt + clay) and the 0.063 to 0.25 mm (fine sand) fractions of till near the bedrock interface and in the 0.063 to 0.25 mm (fine sand) and 0.25 to 0.50 mm (medium sand) fractions in shallow till near surface. The kimberlitic geochemical signature down-ice of the Triple B kimberlite is detectable for till samples containing a minimum of hundreds of indicator minerals in a 10 kg bulk till sample.

IINTRODUCTION

In 2001, shallow trenches were excavated into the Seed kimberlite by the Geological Survey of Canada (GSC). At this time, the Triple B kimberlite was discovered by the GSC while trenching an inferred shallow magnetic bedrock target 240 m east of the Seed kimberlite. In 2002, additional trenching was undertaken on the Triple B kimberlite. GSC Open File 4492 (McClenaghan and Kjarsgaard, 2003) describes the geology of the Seed and Triple B kimberlites, sample collection, and processing methods for the recovery of kimberlite indicator minerals, and visual counts of indicator mineral abundances in the kimberlites and surrounding till. In this report, we present indicator mineral compositions, confirmed by microprobe analysis, for the Seed and Triple B kimberlites, as well as till geochemistry and pebble lithological data from samples adjacent to the Triple B kimberlite.

LOCATION AND ACCESS

The Seed kimberlite is located at latitude 47°26'30"N, longitude 79°41"W (UTM Zone 17, NAD27, Easting 593025, Northing 5256250). The Triple B kimberlite is approximately 240 m to the southeast, located at Easting 5932280, Northing 5256150 (UTM Zone 17, NAD27) (Fig. 1). Both kimberlites are west of the natural gas pipeline and north of South Wabi Creek, in the northeast part of Firstbrook Township, located in a recently logged part of Mr. Jeff Seed's farm.

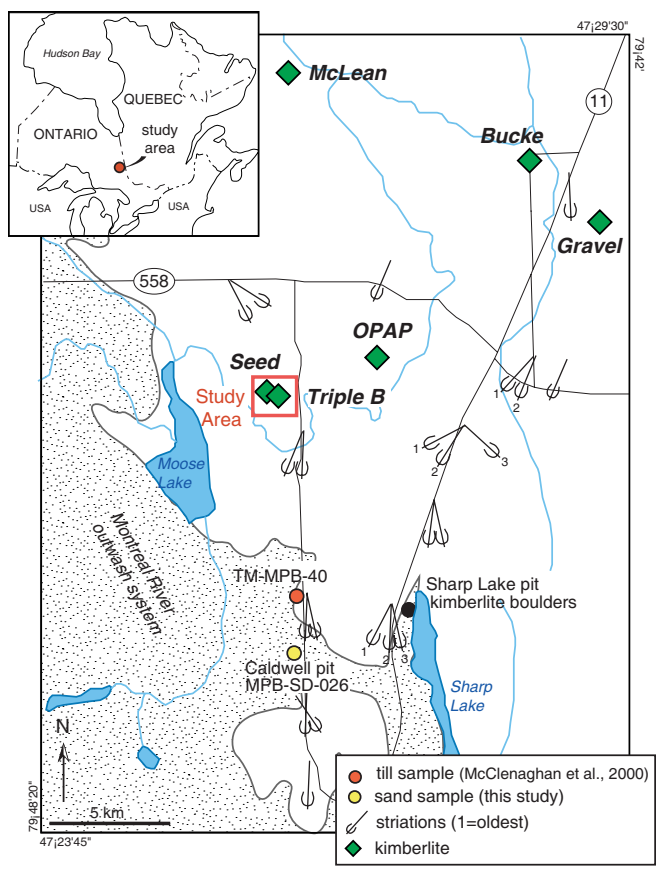

Figure 1. Location of the Seed and Triple B kimberlites, the Caldwell gravel pit and the Sharp Lake pit.

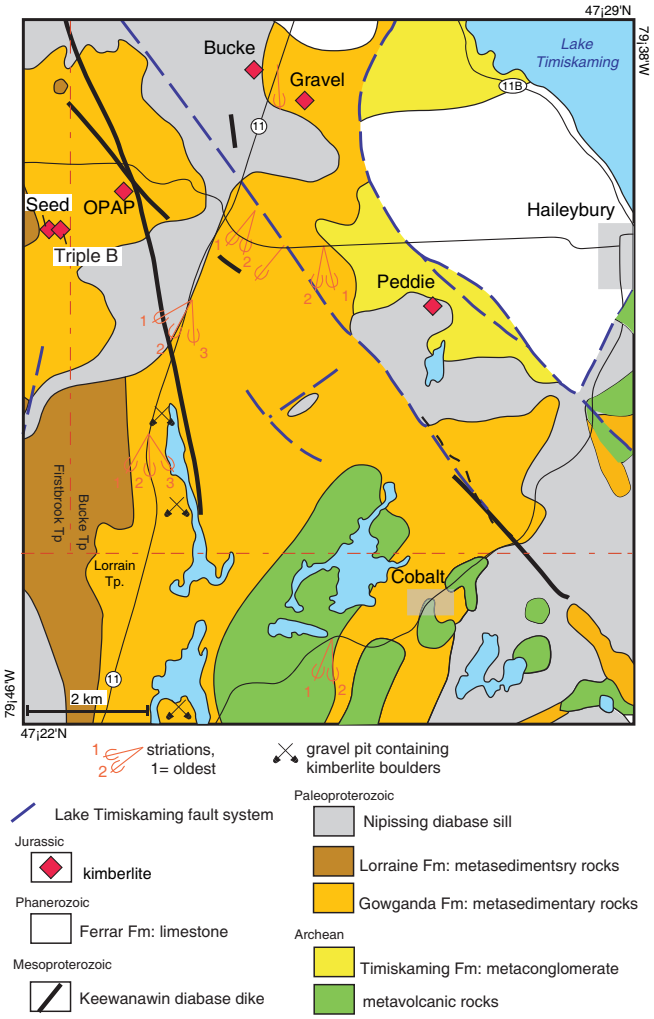

Figure 2. Bedrock geology in the vicinity of the Seed and Triple B kimberlites.

GEOLOGY

Local Bedrock Geology

Bedrock in the vicinity of the kimberlites consists of Paleoproterozoic rocks of the Firstbrook Member of the Gowganda Formation (Fig. 2; Johns and Van Steenburgh, 1984). Paleoproterozoic Nipissing diabase sills intrude the Gowganda Formation, and form extensive areas of outcrop further to the east and north (Fig. 2). Locally, rocks of the Firstbrook Member comprise red to cream/buff, thinly to medium-bedded siltstone and argillite. The Triple B kimberlite intruded argillites of the Firstbrook Member. Although host rock intrusive relationships were not observed in the GSC excavations, the Seed kimberlite is inferred to intrude rocks of the Firstbrook Member. However, a backhoe pit at site SD-025 (Fig. 3) southwest of the uncovered kimberlite (site SD-013), encountered diabase, suggesting the Seed kimberlite also intrudes into Nipissing diabase.

Kimberlite Geology

Seed kimberlite

From studies on drill core, Burgers et al. (1998) described the Seed kimberlite as having variable textures, including transitional pelletal tuffisitic diatreme, globular segregationary hypabyssal, and segregationary hypabyssal kimberlite. Sage (2000) described the Seed kimberlite drill-core samples as a pervasively altered hypabyssal kimberlite. The kimberlite subcrop excavated at sample site SD-013 (Fig. 3, 4) is a pelletal textured kimberlite breccia (>15% clasts larger than 4 mm), with dominantly argillite and limestone and minor diabase clasts. Burgers et al. (1998) describe the hypabyssal Seed kimberlite as a phlogopite and monticellite-bearing calcite kimberlite. Sample SD-013, examined for this study, has a serpentine-rich matrix, with microcrystalline diopside forming at the margins of the pelletal lapilli, which is consistent with "diatreme" kimberlite. A radiometric age of 153.7±1.8 Ma was determined by the U-Pb perovskite technique for the Seed kimberlite (Heaman and Kjarsgaard, 2000). This age suggests the Seed kimberlite is amongst the oldest of the eight Lake Timiskaming field kimberlites dated so far, which vary from 155.4±1.5 Ma (Bucke kimberlite) and 155.3±2.2 Ma (SC 95-2 kimberlite) to 133.9±1.5 Ma (Glinker kimberlite) in age (Heaman and Kjarsgaard, 2000).

The Seed kimberlite has a strong negative magnetic response. The margins of the kimberlite, indicated by the dark blue dashed line in Figure 3, are based on the geology of the subcropping bedrock surface exposed in GSC trenches and the ground magnetic response (McClenaghan and Kjarsgaard, 2003). However, the airborne geophysical anomaly is larger, which indicates the kimberlite body is more extensive at depth (pink dashed line in Fig. 3). The subcropping surface of the kimberlite exposed in the trench is unweathered and striated; no preglacial regolith is present.

Triple B kimberlite

The geology of the Triple B kimberlite is variable. At the northern contact of the main kimberlite body with the Firstbrook argillite (Fig. 5), there is hypabyssal aphanitic kimberlite (about 20 to 30 cm in width), which contains small (<1 mm) olivine phenocrysts, and is almost completely devoid of olivine macrocrysts. Over five metres there is a transition (with increasing olivine macrocryst content) from aphanitic kimberlite to 'normal' looking (i.e. macrocrystic) olivine-rich hypabyssal kimberlite. Approximately 13 m south of the northern contact, there is a significant increase in country rock clasts (limestone and argillite), pelletal lapilli are observed and the matrix is serpentine-rich. Ilmenite and garnet macrocrysts are noticeably abundant in hand samples. This rock is a volcaniclastic (‘diatreme) kimberlite microbreccia. Approximately 16 m south of the northern contact there is a sharp break, south of which the kimberlite is highly altered and light green in colour (Fig. 5). The southern contact of the main Triple B body was not determined; although ground geophysics and trenching suggest the subcropping kimberlite in the trench is about 30 m in width. A narrow kimberlite dyke trending approximately 310° subcrops and was uncovered in two backhoe pits (Fig. 3). This dyke is a hypabyssal phlogopite-spinel-calcite kimberlite, based on petrographic observations. Ilmenite and garnet macrocrysts are noticeably abundant in hand samples of the dyke.

The Triple B kimberlite has a strong negative magnetic response. The outline of the kimberlite, indicated by the blue dashed line in Figure 3, is based on the geology of the sub-

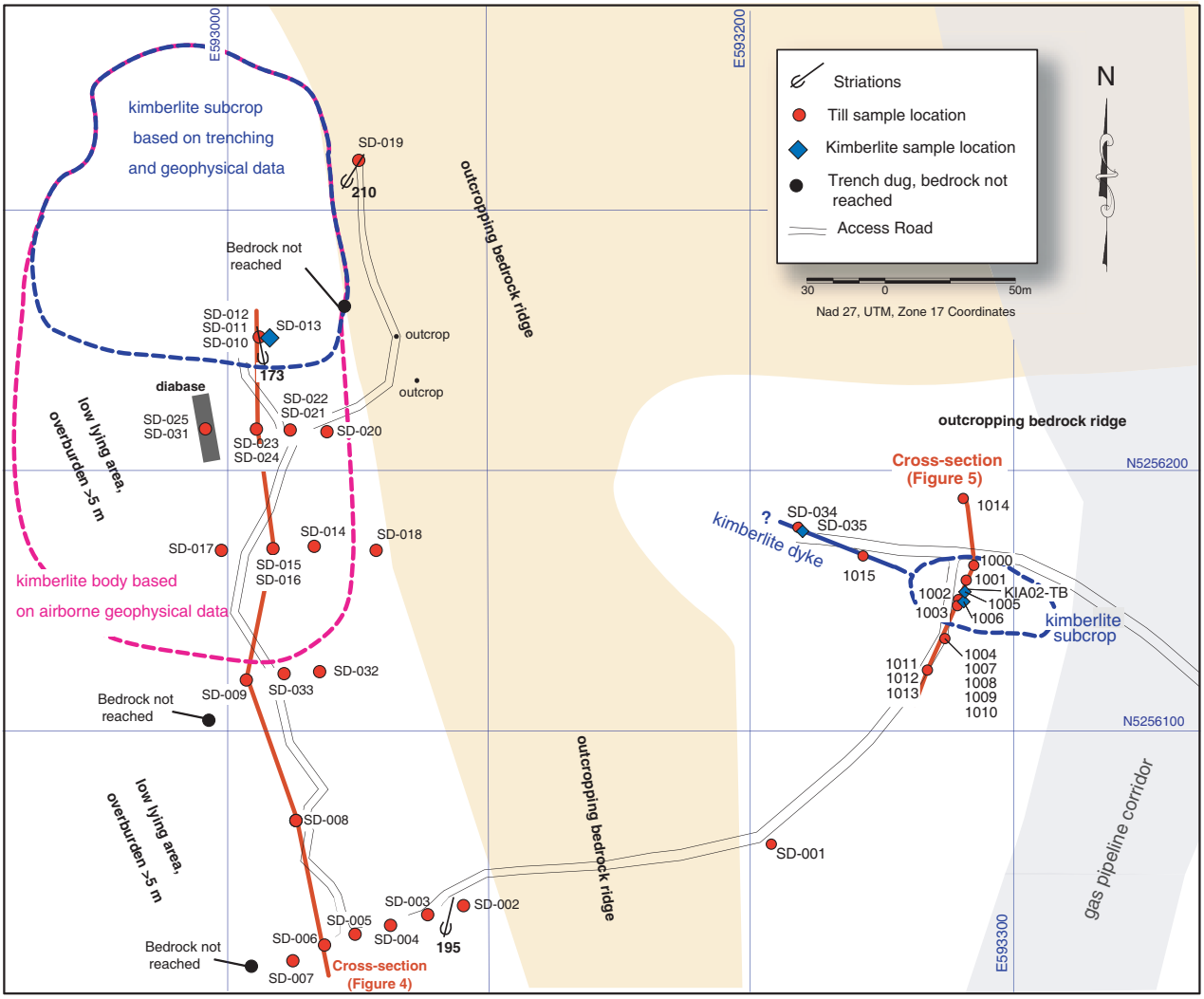

Figure 3. Location of till and kimberlite sample sites around the Seed and Triple B kimberlites. Kimberlite subcrop inferred from geophysical data and trenching outlined by dashed lines.

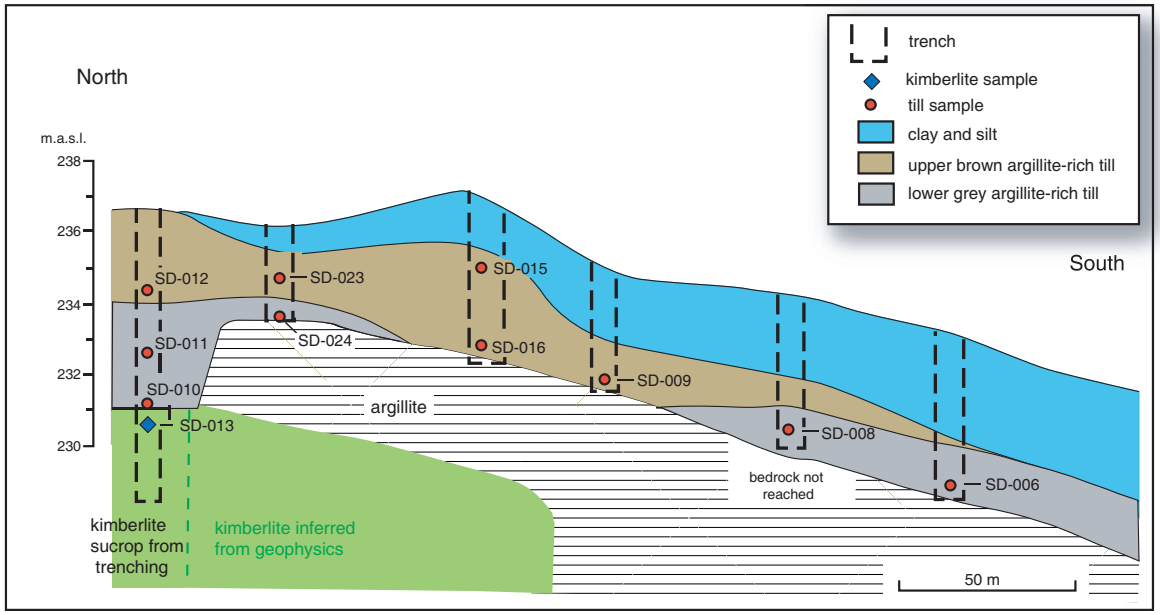

Figure 4. Schematic north-south section over the Seed kimberlite showing glacial sediment thickness and sample locations.

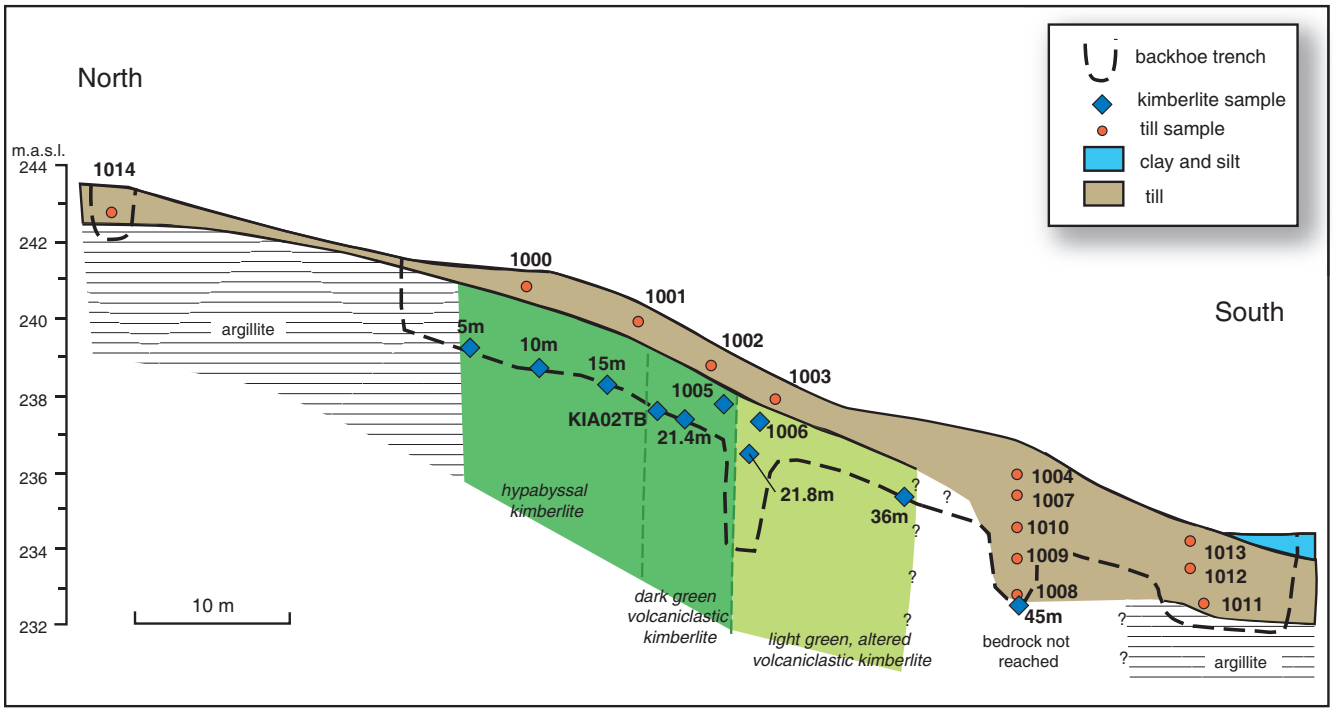

Figure 5. Schematic north-south section over the Triple B kimberlite showing glacial sediment thickness and sample locations.

cropping bedrock surface exposed in GSC trenches and geophysical data. A radiometric age determination for the Triple B kimberlite is currently in progress. The subcropping surface of the kimberlite exposed in the trench is highly weathered and could easily be excavated with a backhoe to at least a 2 m depth. The highly altered volcaniclastic ('diatreme') phase of the kimberlite was easily excavated to a depth of 6 m, throughout which similar highly weathered and friable kimberlite was encountered. The kimberlite dyke was also highly weathered and easily excavated.

Photographs of subcropping kimberlite in the trenches, kimberlite hand-sample slabs, and additional descriptions and figures of the ground magnetic response of the Seed and Triple B kimberlites can be found in Kjarsgaard et al. (2003) and McClenaghan and Kjarsgaard (2003).

Quaternary Geology

Striated bedrock in the area records evidence of three major ice-flow phases (Fig. 1). The oldest flow (Phase 1) was southwestward and likely was associated with the main phase of the Laurentide ice sheet. During deglaciation, ice flow shifted southward (Phase 2). During final deglaciation of the area, local ice tongues from the main ice sheet occupied the structural depressions of the Montreal River and Lake Timiskaming, giving rise to ice flow towards the southeast (Phase 3). All three phases of ice flow are associated with erosion and transportation of kimberlite debris in the region (Veillette, 1986, 1989, 1996; Veillette and McClenaghan, 1996; McClenaghan and Veillette, 2001). The upper surface of the Seed kimberlite is striated towards 173° (Phase 2), although evidence of Phase 1 ice flow is also apparent on bedrock at till sample sites MPB-SD-002 and MPB-SD-019 (Fig. 3) and within the area (Fig. 1).

A schematic north-south cross section across the Seed kimberlite showing glacial sediment thickness is illustrated in Figure 4. The kimberlite is covered by 3 metres of grey, silty sand till which is in turn overlain by 3 metres of brown (oxidized?) silty sand till. West and southwest of the kimberlite, the bedrock surface drops off and till is directly overlain by glaciolacustrine varved clay and silt.

North of, and overlying the north half of, the Triple B kimberlite is a thin veneer (0.5–1.5 m) of brown argillite-rich silty sand till (Fig. 5). Kimberlite fragments as well as bands of greenish brown kimberlite-rich debris (Fig. 6) are common in till overlying the kimberlite. The southern part of the kimberlite is overlain by green kimberlite-rich silty sand till. South of the kimberlite, the bedrock surface drops off dramatically, and the green till is overlain by 1 to 3 metres of glaciolacustrine varved clay and silt.

METHODS

Sample Collection and Preparation

Sample collection, preparation, and processing procedures and the weight of fractions produced during the recovery of indicator minerals from the Seed and Triple B kimberlites and surrounding till samples were reported in McClenaghan and Kjarsgaard (2003). Samples were collected from both kimberlites for indicator mineral analysis. One volcaniclastic ('diatreme') kimberlite sample was collected from the Seed kimberlite (sample MPB-SD-013). Four kimberlite samples representing three of the four observed phases observed at Triple B were collected: a) dark green volcaniclastic ('diatreme') kimberlite (samples MPB-02-1005, K1A02-TB) from the central part of the kimberlite; b) light green (highly altered) volcaniclastic ('diatreme') kimberlite (sample MPB-02-1006) from the south part of the kimberlite; and c) hypabyssal kimberlite from the Triple B dyke,

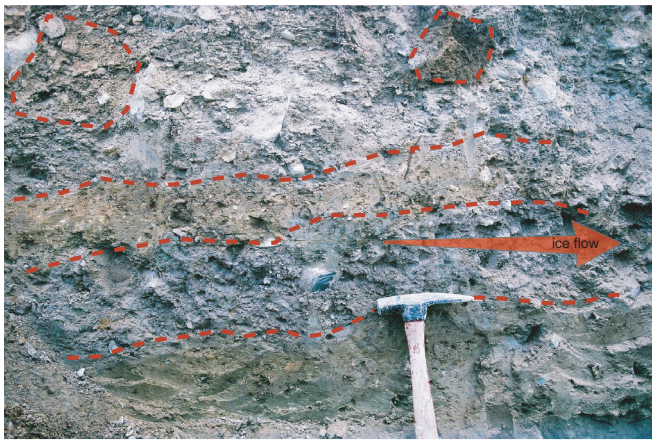

Figure 6. Bands of kimberlite-rich till (yellowish-green-brown) and a kimberlite cobble within kimberlite-poor grey till overlying the Triple B kimberlite. Note hammer for scale.

west of the main kimberlite (sample MPB-SD-035). Till samples were collected from shallow trenches excavated north of, overlying, and down-ice of both the Seed and Triple B kimberlites. Samples MPB-SD-001 to MPB-SD-035 were collected in 2001 and samples MPB-02-1000 to MPB-02-1015 were collected in 2002 (Fig. 2). Location and descriptive information for each sample are listed in Appendix A. In addition, one sand sample (MPB-SD-026) was collected from glaciofluvial deposits in the Caldwell gravel pit approximately 3 km south of the kimberlites (Fig. 1).

Samples were processed at Overburden Drilling Management Ltd. to prepare non-ferromagnetic heavy mineral concentrates for the 0.25 to 0.5 mm, 0.5 to 1.0 mm, and 1.0 to 2.0 mm fraction of kimberlite and till. During sample processing, the >2.0 mm (+10 mesh) material of till samples was retained and examined by Consorminex Inc., Gatineau, Quebec for analysis of pebble lithologies. Approximately 200 clasts from the 0.8 to 5 cm (pebble) fraction were screened and classified into categories that reflect the major rock types in the region: felsic to intermediate intrusive, mafic intrusive, ultramafic intrusive, metavolcanic, metasedimentary, Huronian metasediments, Paleozoic carbonate, kimberlite, and other or unknown rock types. Pebble abundances (listed as frequency %) for till around the Seed and Triple B kimberlites are reported in Appendix B.1. A digital colour photograph of the pebble fraction of each till sample is included in Appendix B.2.

Kimberlite Indicator Mineral Identification

The three size fractions of heavy minerals were examined by I. & M. Morrison Geological Services, Delta, B.C., using stereoscopic and petrographic microscopes and potential kimberlite indicator minerals were counted and set aside for microprobe analysis. Indicator minerals were visually selected on the basis of physical properties, such as colour, grain morphology, and/or the presence of adhering kimberlite matrix material (e.g. Muggeridge, 1995). Minerals picked included purple Cr-pyrope, red titanian Cr-poor pyrope (megacryst garnet), orange Mg-almandine (eclogitic garnet), green Cr-diopside, black Mg-ilmenite and chromite, and pale yellow olivine. Although enstatite and perovskite were not targeted, they were picked from the concentrates and analyzed because they resembled olivine, Mg-ilmenite, or chromite, respectively. Picked grains were mounted in 25 mm epoxy mounts and polished at Lakefield Research, Lakefield, Ontario in preparation for electron microprobe analysis to confirm their identity and further classify them using mineral chemistry. Electron microprobe analyses were carried out at the GSC using operating conditions and mineral sorting routines similar to those described by McClenaghan et al. (1999) and microprobe data are listed in Appendix C. Abundances of pyrope reported in Table 1 reflect the sum of Cr-pyrope and pyrope grains in each sample, and abundances of the two will be referred to collectively in this report as pyrope.

Preliminary kimberlite indicator mineral abundances determined by visual identification reported in GSC Open File 4492 (McClenaghan and Kjarsgaard, 2003) are listed in Appendix D. The abundances were confirmed by microprobe analysis for most samples. For samples that contained hundreds to thousands of indicator minerals, a selection of indicator minerals were analysed to establish the compositional range of each mineral species, as well as determine the success rate (correction factor) of the visual identification (Appendix D). Indicator mineral counts were then corrected to reflect the number of grains for which identification was either confirmed by microprobe analysis or adjusted using the correction factors. The correction factors were calculated by comparing the number of grains correctly identified and confirmed by microprobe analysis to the number picked. For example, the correction factor for Triple B Mg-ilmenite is 60%, indicating that for 60% of the Mg-ilmenite picked as potential Mg-ilmenite, approximately 60% were confirmed by microprobe analysis to be Mg-ilmenite. The other 40% of the grains picked were ilmenite, chromite, or Fe-Ti oxides. Corrected counts were then normalized to a 10 kg sample weight (Appendix D) and these normalized grain counts are reported in Table 1.

Geochemical Analysis of Kimberlite and Till

Two samples of the Seed kimberlite, four samples of the Triple B kimberlite dyke and four samples of the Triple kimberlite pipe were analyzed for major, minor, and trace elements. Fourteen till samples and two kimberlite samples from the Triple B kimberlite were analyzed in a separate batch. Only till from the Triple B kimberlite was geochemically analyzed, as till around the Seed kimberlite contained few to no kimberlite pebbles or indicator minerals. A 250 g split of the till samples collected around the Triple B kimberlite was prepared by the GSC Sedimentology Laboratory, Ottawa. Samples were oven dried at <40°C and sieved into four sub-fractions for geochemical analysis: 1) <0.063 mm (silt+clay); 2) 0.063 to 0.25 mm (fine sand); 3) 0.25 to 0.5 mm (medium sand); and 4) 0.5 to 2.0 mm (coarse to very coarse sand).

Geochemical analyses of kimberlite and till were performed at ACME Labs, Vancouver, BC, using the following methods: 1) major elements by $LiBO_2$ fusion/ICP-ES, C and S by Leco, LOI by loss on ignition (package 4A); 2) minor and trace elements by $LiBO_2$ fusion/ICP-MS (package 4B); and 3) precious and base metals by aqua regia/ICP-MS (package 1DX). Elements determined, analytical methods,

Table 1. Kimberlite indicator mineral abundance normalized to 10 kg samples weight for kimberlite, till, and sand samples around the Seed (from Appendix D.1) and Triple B (from Appendix D.2) kimberlites.

a) Seed kimberlite

SAMPLE	KIMBERLITE	MATERIAL TYPE	WEIGHT <2mm (kg)	0.25 to 0.5 mm						0.5 to 1.0 mm						1.0 to 2.0 mm					
				PYR	ECL	CD	ILM	CHR	OLV	PY	ECL	CD	ILM	CHR	OLV	PY	ECL	CD	ILM	CHR	OLV
MPB-SD-002	Seed	till	3.8	8	0	13	42	16	0	0	0	3	8	0	0	0	0	0	0	0	0
MPB-SD-003	Seed	till	7.4	0	0	3	0	0	0	0	0	0	0	0	0	0	0	0	0	0	0
MPB-SD-004	Seed	till	5.9	0	0	0	0	0	0	0	0	0	0	0	0	0	0	0	0	0	0
MPB-SD-005	Seed	till	5.2	0	0	0	0	0	0	0	0	0	0	0	0	0	0	0	0	0	0
MPB-SD-006	Seed	till	8.0	0	0	4	0	0	0	0	0	0	0	0	0	0	0	0	0	0	0
MPB-SD-007	Seed	till	9.6	5	0	16	4	2	0	1	0	0	2	0	0	0	0	0	0	0	0
MPB-SD-008	Seed	till	6.2	0	0	5	0	0	0	0	0	0	0	0	0	0	0	0	0	0	0
MPB-SD-009	Seed	till	6.9	6	0	22	23	0	0	0	0	0	4	0	0	0	0	0	1	0	0
MPB-SD-010	Seed	till	11.0	2	0	6	12	2	0	0	0	1	7	1	0	0	0	0	2	0	0
MPB-SD-011	Seed	till	7.6	0	0	13	0	1	0	0	0	0	0	0	0	0	0	0	0	0	0
MPB-SD-012	Seed	till	6.6	0	0	3	0	0	0	0	0	0	0	0	0	0	0	0	0	0	0
MPB-SD-013	Seed	kimberlite	10.0	133	0	59	3653	5	0	5	0	4	1890	2	0	3	0	0	591	0	0
MPB-SD-014	Seed	till	7.8	4	0	24	13	8	0	0	0	0	4	1	0	0	0	0	0	0	0
MPB-SD-015	Seed	till	8.9	8	0	21	19	2	0	2	0	1	6	0	0	1	0	0	1	0	0
MPB-SD-016	Seed	till	7.8	4	0	17	18	1	0	0	0	0	5	0	0	0	0	0	1	0	0
MPB-SD-017	Seed	till	9.9	10	0	15	16	2	0	1	0	0	4	1	0	0	0	0	0	0	0
MPB-SD-018	Seed	till	5.9	7	0	24	29	3	0	0	0	0	2	0	0	0	0	0	2	0	0
MPB-SD-019	Seed	till	5.8	2	0	50	12	2	0	0	0	0	2	0	0	0	0	0	0	0	0
MPB-SD-020	Seed	till	6.8	9	0	10	16	6	0	0	0	0	4	0	0	0	0	0	0	0	0
MPB-SD-021	Seed	till	6.6	2	0	0	0	2	0	0	0	0	0	0	0	0	0	0	0	0	0
MPB-SD-022	Seed	till	7.4	0	0	7	0	0	0	0	0	0	0	0	0	0	0	0	0	0	0
MPB-SD-023	Seed	till	8.3	2	0	7	10	7	0	0	0	0	1	1	0	0	0	0	0	0	0
MPB-SD-024	Seed	till	6.0	0	0	3	0	0	0	0	0	0	0	0	0	0	0	0	0	0	0
MPB-SD-025	Seed	till	7.5	1	0	4	5	1	0	0	0	0	0	0	0	0	0	0	0	0	0
MPB-SD-026	Seed	sand	3.3	21	0	12	36	21	12	12	0	0	48	3	48	0	0	0	0	0	6
MPB-SD-031	Seed	till	7.1	0	0	1	0	0	0	0	0	0	0	0	0	0	0	0	0	0	0
MPB-SD-032	Seed	till	7.7	0	0	9	6	0	0	0	0	0	3	0	0	0	0	0	0	0	0
MPB-SD-033	Seed	till	7.3	1	0	22	23	10	1	0	0	1	5	0	0	0	0	0	0	0	0

b) Triple B kimberlite

SAMPLE	KIMBERLITE	MATERIAL TYPE	WEIGHT <2mm (kg)	0.25 to 0.5 mm						0.5 to 1.0 mm						1.0 to 2.0 mm					
				PYR	ECL	CD	ILM	CHR	OLV	PYR	ECL	CD	ILM	CHR	OLV	PYR	ECL	CD	ILM	CHR	OLV
SD-001	Triple B	till	7.9	0	0	0	8	3	0	0	0	1	1	0	1	0	0	0	0	0	0
MPB-02-1000	Triple B	till	4.5	4	0	0	9	9	7	0	0	0	2	2	2	0	0	0	2	0	0
MPB-02-1001	Triple B	till	5.4	6	0	0	26	2	8	0	0	0	13	0	0	0	0	0	0	0	0
MPB-02-1002	Triple B	till	5.6	20	0	14	84	4	342	0	0	2	9	0	38	0	0	0	4	0	0
MPB-02-1003	Triple B	till	5.1	0	0	8	51	4	55	0	0	0	0	0	4	0	0	0	4	0	0
MPB-02-1004	Triple B	till	5.5	33	0	91	138	13	125	5	0	2	56	15	20	0	0	0	18	0	0
MPB-02-1005	Triple B	dark green kimberlite	5.7	142	0	295	533	54	21	58	0	77	235	28	53	12	0	2	132	2	0
MPB-02-1006	Triple B	light green kimberlite	5.3	409	0	300	3557	34	23	83	0	55	766	6	4	26	0	0	233	4	0
MPB-02-1007	Triple B	till	5.6	239	0	305	3845	13	339	70	0	79	1080	0	41	2	0	4	136	0	0
MPB-02-1008	Triple B	till	8.6	135	0	223	3756	22	13	59	0	48	928	8	3	8	0	5	175	0	0
MPB-02-1009	Triple B	till	6.3	233	0	251	4381	103	16	84	0	43	1844	41	2	11	0	0	153	2	0
MPB-02-1010	Triple B	till	5.7	298	0	409	4611	105	16	72	0	51	940	26	4	2	0	4	116	4	2
MPB-02-1011	Triple B	till	6.7	148	0	263	3134	36	1166	75	0	49	278	24	222	10	0	0	169	1	0
MPB-02-1012	Triple B	till	3.9	238	0	444	3821	77	37	85	0	67	454	69	10	8	0	0	168	5	3
MPB-02-1013	Triple B	till	4.5	24	0	93	1118	18	886	11	0	13	64	16	138	0	0	0	16	0	0
MPB-02-1014	Triple B	till	5.7	5	0	35	11	2	4	0	0	0	0	0	0	0	0	0	0	0	0
MPB-02-1015	Triple B	till	5.9	185	0	24	217	7	93	17	0	3	32	2	3	0	0	0	5	0	0
SD-034	Triple B	till	6.4	52	0	0	28	0	0	3	0	0	14	0	0	0	0	0	3	0	0
SD-035	Triple B	kimberlite dyke	5.5	905	0	27	2978	24	0	364	0	4	739	11	0	111	0	0	256	5	0
K1A02-TB	Triple B	kimberlite	15.5	101	0	121	1742	2	22	12	0	22	2787	2	8	0	0	0	7	0	0

and lower detection limits are listed in Table 2 and the geochemical data are listed in Appendix E. Analytical accuracy for till samples was monitored by analyzing CANMET certified reference standards MRG-1 (Govindaraju, 1994), UM-2 (www.nrcan.gc.ca/mms/canmet-mtb/mmsl-lmsm/ccrmp/certificates/um-2.htm) and SY-22(www.nrcan.gc.ca/mms/canmet-mtb/mmsl-lmsm/ccrmp/certificates/sy-4.htm) (Table 3, Appendix E). Analytical precision for till samples was monitored by comparing analyses of split duplicates (GSC sample lab prepared and ACME splits). All quality control data are reported in Appendix E.

KIMBERLITE INDICATOR MINERAL ABUNDANCE

Seed Kimberlite

The kimberlite indicator mineral suite in the Seed kimberlite (sample MPB-SD-013) is dominated by Mg-ilmenite (1000s of grains) followed in decreasing order of abundance, by pyrope (100s of grains), Cr-diopside (10s of grains), and chromite (a few grains) (Table 1, Fig. 7). Olivine was not found in sample MPB-SD-013, consistent with observations that olivine in the Seed kimberlite has been completely altered to serpentine (Sage, 2000; Kjarsgaard et al., 2003). Indicator minerals are most abundant, by far, in the 0.25 to 0.5 mm fraction.

Most till samples collected around the Seed kimberlite contain Mg-ilmenite, low-MgO (crustal) ilmenite and Cr-diopside in about equal proportions, whereas pyrope garnet and chromite are much less abundant. Notable exceptions are sample MPB-SD-019, collected up-ice from Seed (representing ‘background’ concentrations), which contains abundant Cr-diopside but few other kimberlite indicator minerals, and glaciofluvial sand sample MPB-SD-026 from the Caldwell gravel pit, which contains mostly Mg-ilmenite and olivine. Ten-kg till samples down-ice from the Seed kimberlite contain between 0 and 42 Mg-ilmenite (Fig. 8a), 0 to 10 pyrope (Fig. 8b), 0 to 50 Cr-diopside (Fig. 8c), and 0 to 16

Table 2. Analytical methods and lower detection limits for geochemical analysis of Triple B till samples.

Element	Unit of measure	Method	Lower detection limit	Lab	ACME File Number
SiO_2	%	$LiBO_2$ fusion/ICP-ES	0.00	ACME	A300498
Al_2O_3	%	$LiBO_2$ fusion/ICP-ES	0.00	ACME	A300498
Fe_2O_3	%	$LiBO_2$ fusion/ICP-ES	0.00	ACME	A300498
MgO	%	$LiBO_2$ fusion/ICP-ES	0.00	ACME	A300498
CaO	%	$LiBO_2$ fusion/ICP-ES	0.00	ACME	A300498
Na_2O	%	$LiBO_2$ fusion/ICP-ES	0.00	ACME	A300498
K_2O	%	$LiBO_2$ fusion/ICP-ES	0.00	ACME	A300498
TiO_2	%	$LiBO_2$ fusion/ICP-ES	0.00	ACME	A300498
P_2O_5	%	$LiBO_2$ fusion/ICP-ES	0.00	ACME	A300498
MnO	%	$LiBO_2$ fusion/ICP-ES	0.00	ACME	A300498
Cr_2O_3	%	$LiBO_2$ fusion/ICP-ES	0.001%	ACME	A300498
Ba	ppm	$LiBO_2$ fusion/ICP-ES	5 ppm	ACME	A300498
Ni	ppm	$LiBO_2$ fusion/ICP-ES	30 ppm	ACME	A300498
Sc	ppm	$LiBO_2$ fusion/ICP-ES	1 ppm	ACME	A300498
LOI	%	Loss on ignition	0.00	ACME	A300498
TOT/C	%	Leco	0.00	ACME	A300498
TOT/S	%	Leco	0.00	ACME	A300498
Co	ppm	$LiBO_2$ fusion/ICP-ES	0.5	ACME	A300498A
Cs	ppm	$LiBO_2$ fusion/ICP-ES	0.1	ACME	A300498A
Ga	ppm	$LiBO_2$ fusion/ICP-ES	0.5	ACME	A300498A
Hf	ppm	$LiBO_2$ fusion/ICP-ES	0.5	ACME	A300498A
Nb	ppm	$LiBO_2$ fusion/ICP-ES	0.5	ACME	A300498A
Rb	ppm	$LiBO_2$ fusion/ICP-ES	0.5	ACME	A300498A
Sn	ppm	$LiBO_2$ fusion/ICP-ES	1	ACME	A300498A
Sr	ppm	$LiBO_2$ fusion/ICP-ES	0.5	ACME	A300498A
Ta	ppm	$LiBO_2$ fusion/ICP-ES	0.1	ACME	A300498A
Th	ppm	$LiBO_2$ fusion/ICP-ES	0.1	ACME	A300498A
U	ppm	$LiBO_2$ fusion/ICP-ES	0.1	ACME	A300498A
V	ppm	$LiBO_2$ fusion/ICP-ES	5	ACME	A300498A
W	ppm	$LiBO_2$ fusion/ICP-ES	0.1	ACME	A300498A
Zr	ppm	$LiBO_2$ fusion/ICP-ES	0.5	ACME	A300498A
Y	ppm	$LiBO_2$ fusion/ICP-ES	0.1	ACME	A300498A
La	ppm	$LiBO_2$ fusion/ICP-ES	0.5	ACME	A300498A
Ce	ppm	$LiBO_2$ fusion/ICP-ES	0.5	ACME	A300498A
Pr	ppm	$LiBO_2$ fusion/ICP-ES	0.02	ACME	A300498A
Nd	ppm	$LiBO_2$ fusion/ICP-ES	0.4	ACME	A300498A
Sm	ppm	$LiBO_2$ fusion/ICP-ES	0.1	ACME	A300498A
Eu	ppm	$LiBO_2$ fusion/ICP-ES	0.05	ACME	A300498A
Gd	ppm	$LiBO_2$ fusion/ICP-ES	0.05	ACME	A300498A
Tb	ppm	$LiBO_2$ fusion/ICP-ES	0.01	ACME	A300498A
Dy	ppm	$LiBO_2$ fusion/ICP-ES	0.05	ACME	A300498A
Ho	ppm	$LiBO_2$ fusion/ICP-ES	0.05	ACME	A300498A
Er	ppm	$LiBO_2$ fusion/ICP-ES	0.05	ACME	A300498A
Tm	ppm	$LiBO_2$ fusion/ICP-ES	0.05	ACME	A300498A
Yb	ppm	$LiBO_2$ fusion/ICP-ES	0.05	ACME	A300498A
Lu	ppm	$LiBO_2$ fusion/ICP-ES	0.01	ACME	A300498A
Mo	ppm	HCl-HNO_2 (2:2) ICP-MS	0.0	ACME	A300498B
Cu	ppm	HCl-HNO_2 (2:2) ICP-MS	0.1	ACME	A300498B
Pb	ppm	HCl-HNO_2 (2:2) ICP-MS	0.1	ACME	A300498B
Zn	ppm	HCl-HNO_2 (2:2) ICP-MS	1	ACME	A300498B
Ni	ppm	HCl-HNO_2 (2:2) ICP-MS	0.1	ACME	A300498B
As	ppm	HCl-HNO_2 (2:2) ICP-MS	0.5	ACME	A300498B
Cd	ppm	HCl-HNO_2 (2:2) ICP-MS	0.1	ACME	A300498B
Sb	ppm	HCl-HNO_2 (2:2) ICP-MS	0.1	ACME	A300498B
Bi	ppm	HCl-HNO_2 (2:2) ICP-MS	0.1	ACME	A300498B
Ag	ppm	HCl-HNO_2 (2:2) ICP-MS	0.1	ACME	A300498B
Au	ppb	HCl-HNO_2 (2:2) ICP-MS	0.5	ACME	A300498B
Hg	ppm	HCl-HNO_2 (2:2) ICP-MS	0.01	ACME	A300498B
Tl	ppm	HCl-HNO_2 (2:2) ICP-MS	0.1	ACME	A300498B

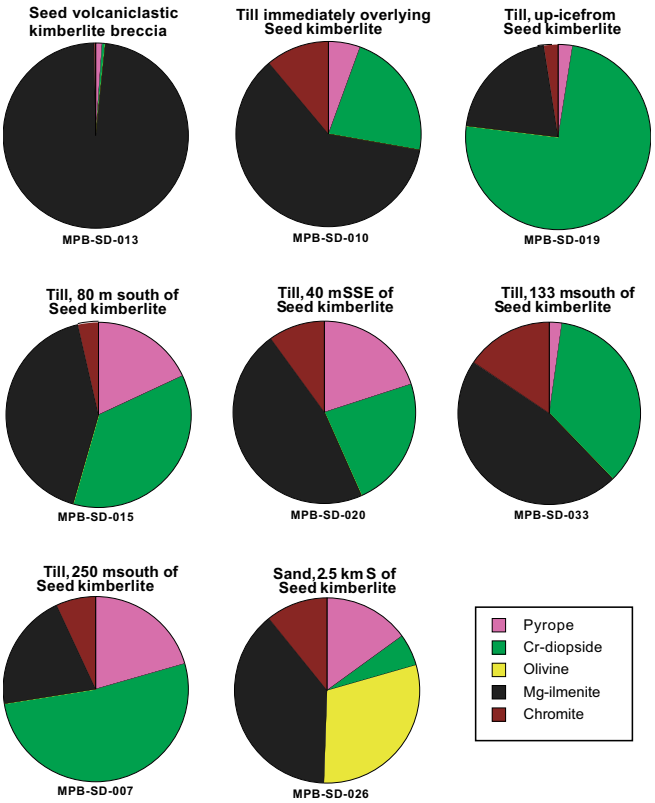

Figure 7. Proportional pie plots of the relative abundance of Mg-ilmenite, pyrope, Cr-diopside, olivine and chromite in the 0.25 to 0.5 mm fraction of the Seed kimberlite and till samples.

chromite grains (Fig. 8d). Nine till samples contain no indicator minerals except a few grains of Cr-diopside (Fig. 8c).

Enstatite was only found in till sample SD-010 collected directly overlying the Seed kimberlite, which also contains enstatite. In addition, other non-kimberlite indicator minerals found in the till samples that were picked and probed because they resembled kimberlite indicator minerals include: hematite, rutile, and non-stoichiometric Fe-Ti-oxide (all three alteration products of ilmenite or Ti-magnetite), melanite garnet (Ti-rich black to brown andradite garnet), staurolite, amphibole, epidote, almandine-spessartine, grossular, andradite, and zircon.

Triple B Kimberlite

The three samples of the main kimberlite body are characterized by abundant Mg-ilmenite (1000s of grains) similar to the Seed kimberlite, followed in decreasing order of abundance by Cr-diopside (100s of grains), pyrope (100s of grains), chromite 10s of grains) and olivine (10s of grains) (Fig. 9, Table 1). The kimberlite dyke (MPB-SD-035) contains a higher proportion of pyrope but fewer Cr-diopside and chromite than the main kimberlite body (Table 1) and no olivine. Petrographic examination of twenty representative Triple B kimberlite thin sections (main body hypabyssal and volcaniclastic, and dyke) indicates that: 1) olivine in the dyke has been completely altered to serpentine; 2) in the main Triple B body, alteration of olivine to serpentine shows variable stages, for a number of samples all the olivine is completely replaced by serpentine; and in a subset of the samples, a few cores of macrocrysts, as well as a small per-

Table 3. List of recommended values for certified reference standards MRG-1, SY-4, and UM-2 and values obtained in this study.

ELEMENT	MRG-1 Certified standard (%)	GSC data (%) N=2	SY-4 Certified standard (%)	GSC data (%) N=1	UM-2 Certified standard (%)	GSC data (%) N=1
SiO_2	39.12	38.9	**49.9**	50.05	39.2	39.98
Al_2O_3	8.47	8.38	20.69	20.52	7.23	7.18
Fe_2O_3t	17.94	17.86	6.21	6.33	12.95	13.24
FeO	not reported	not reported	2.86	not reported	not reported	not reported
MgO	13.55	13.58	0.54	0.61	25.45	24.55
CaO	14.7	14.81	8.05	8.38	4.68	4.78
Na_2O	0.47	0.68	7.1	6.84	0.32	0.28
K_2O	0.18	0.18	1.66	1.61	0.11	0.05
TiO_2	3.77	3.93	0.287	0.29	0.24	0.24
P_2O_5	0.08	0.11	0.131	0.12	0.02	0.06
MnO	0.17	0.16	0.108	0.10	0.08	0.06
Cr_2O_3	not reported	0.06	not reported	0.00	1.51	1.281
LOI	1.56	1.3	4.56	4.9	not reported	7.7
TOT/C	not reported	0.33	1	1.1	not reported	0.04
TOT/S	not reported	0.07	0.015	0.01	0.94	1.09

ELEMENT	MRG-1 certified standard ppm)	GSC data (ppm)	SY-4 Certified standard (ppm)	GSC data (ppm)	UM-2 Certified standard ppm)	GSC data (ppm)
Ba	61	52	340	328	not reported	not reported
Co	87	89	2.8	1.3	120	175.6
Cs	0.57	0.55	1.5	1.4	not reported	not reported
Ga	17	20	35	39.3	not reported	not reported
Hf	3.76	3.95	10.6	11.0	not reported	not reported
Nb	20	21	13	13.6	not reported	not reported
Ni	193	194	9	< 20	not reported	not reported
Rb	8.5	7.1	55	52.8	not reported	not reported
Sc	55	54.5	1.1	1.0	not reported	not reported
Sn	4.5	5.0	7.1	8.0	not reported	not reported
Sr	266	284	1191	1244	not reported	not reported
Ta	0.8	0.9	0.9	1.1	not reported	not reported
Th	0.93	1.2	1.4	1.6	not reported	not reported
U	0.24	0.35	0.8	1.0	not reported	not reported
V	526	548	8	5.0	not reported	not reported
W	0.3	0.23	0.2-15	< .1	not reported	not reported
Zr	108	100	517	538	not reported	not reported
Y	14	13	119	137	not reported	not reported
La	9.8	10	58	63	not reported	not reported
Ce	26	29	122	123	not reported	not reported
Pr	3.4	3.98	15	15	not reported	not reported
Nd	19.2	18.5	57	57	not reported	not reported
Sm	4.5	4.7	12.7	14.0	not reported	not reported
Eu	1.39	1.515	2.99	2.2	not reported	not reported
Gd	4	4.26	14	16.4	not reported	not reported
Tb	0.51	0.58	2.6	2.9	not reported	not reported
Dy	2.9	3.16	18.2	19.3	not reported	not reported
Ho	0.49	0.52	4.3	4.6	not reported	not reported
Er	1.12	1.27	14.2	13.8	not reported	not reported
Tm	0.11	0.16	2.3	2.4	not reported	not reported
Yb	0.6	0.91	14.8	16.0	not reported	not reported
Lu	0.12	0.14	2.1	2.2	not reported	not reported
Mo	0.87	0.95	0.2-3	0.2	not reported	not reported
Cu	134	118.9	7	2.7	950	953.5
Pb	10	4.2	10	1.8	not reported	not reported
Zn	191	120.5	93	49	not reported	not reported
Ni	193	124.5	9	5.3	2900	2660.2
As	0.73	<0.5	0.1-2	<0.5	not reported	not reported
Cd	0.168	0.1	0.1-2	0.1	not reported	not reported
Sb	0.86	0.2	0.01-0.3	<0.1	not reported	not reported
Bi	0.13	0.1	0.1-0.3	<0.1	not reported	not reported
Ag	0.11	0.1	0.6	<0.1	not reported	not reported
Au (ppb)	5.4	6.45	not reported	<0.5	not reported	not reported
Hg	0.14	0.09	10-14	<0.01	not reported	not reported
Tl	0.055	<0.1	0.2-0.5	0.2	not reported	not reported

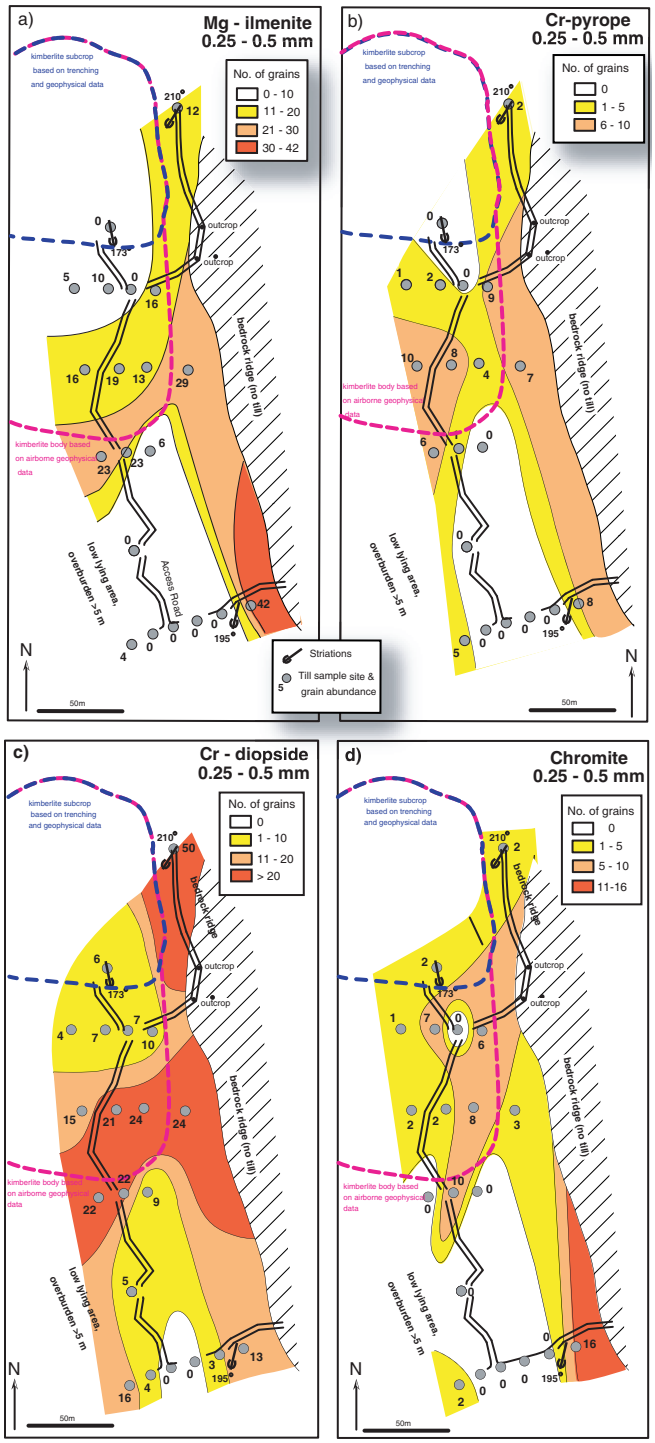

Figure 8. Number of indicator minerals normalized to 10 kg sample weight, in the 0.25 to 0.5 mm fraction of surface till samples around the Seed kimberlite: **a)** Mg-ilmenite; **b)** pyrope; **c)** Cr-diopside; and **d)** chromite.

centage of the olivine phenocrysts remain unaltered. No eclogitic garnet was found in either the main kimberlite body or the dyke. Indicator minerals are concentrated in the smallest (0.25-0.5 mm) size fraction; however, they are far more abundant in the two coarser fractions than for the Seed kimberlite (Table 1).

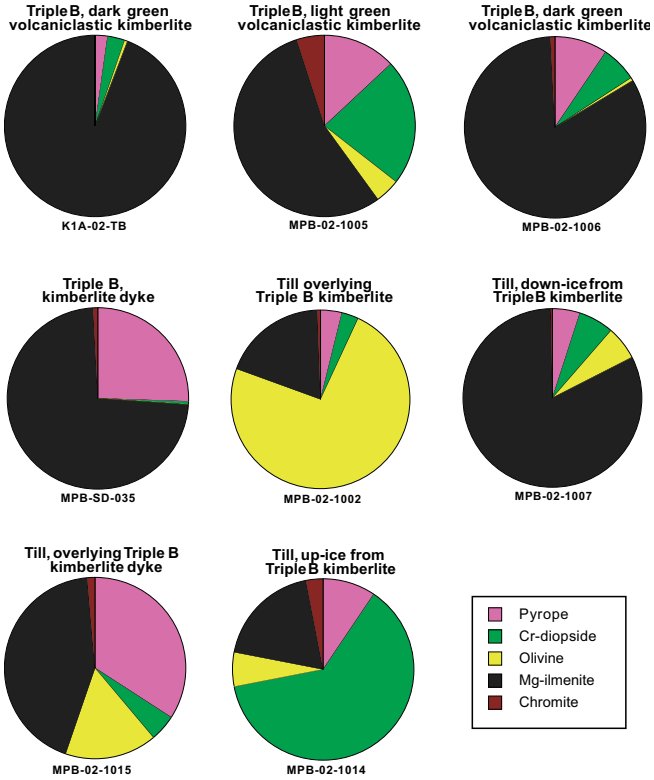

Figure 9. Proportional pie plots of the relative abundance of Mg-ilmenite, Pyrope, Cr-diopside, olivine and chromite in the 0.25 to 0.5 mm fraction of the three phases Triple B kimberlite body, Triple B dyke, and till samples.

Till samples collected from trenches up-ice (sample MPB-02-014), overlying (sample MPB-02-1000), and 100 m southwest (sample MPB-SD-001) of the kimberlite contain only a few indicator minerals (Table 1). These low values reflect background concentrations of indicator minerals in till near the Triple B kimberlite (pyrope = 5; eclogitic garnet = 0; Cr-diopside = 35; Mg-ilmenite = 11, chromite = 9, and olivine = 7). Till samples MPB-02-1001 to MPB-02-1003, overlying the kimberlite, contain slightly elevated abundances of Mg-ilmenite and olivine (Fig. 10, Table 1) reflecting minor incorporation of kimberlite debris in the till. Till samples MPB-02-1004 to MPB-02-1013, down-ice from the kimberlite and sample MPB-02-1015 overlying the kimberlite dyke, contain thousands of indicator minerals with mineral species occurring in relative proportions similar to the main kimberlite body and dyke respectively (Table 1). Indicator minerals in the 0.25 to 0.5 mm fraction of till down-ice are dominated by Mg-ilmenite (1000s of grains) (Fig. 10a), followed by garnet (Fig. 10b) and Cr-diopside (100s of grains) and few chromite (10s of grains). In contrast to the three Triple B kimberlite samples, till samples 1002, 1004, 1007, 1011, 1013, and 1015 contain abundant olivine (>100 grains/10 kg) (Fig. 10c).

As a kimberlite groundmass mineral, perovskite is commonly too small to be included in indicator mineral studies. In some samples, however, large (>0.25 mm) perovskite grains were mistakenly picked as Mg-ilmenite grains and analyzed. A total of 67 perovskite grains were (accidentally) picked from the three size fractions of the Triple B kimberlite. Two perovskite grains were picked in the Triple B dyke

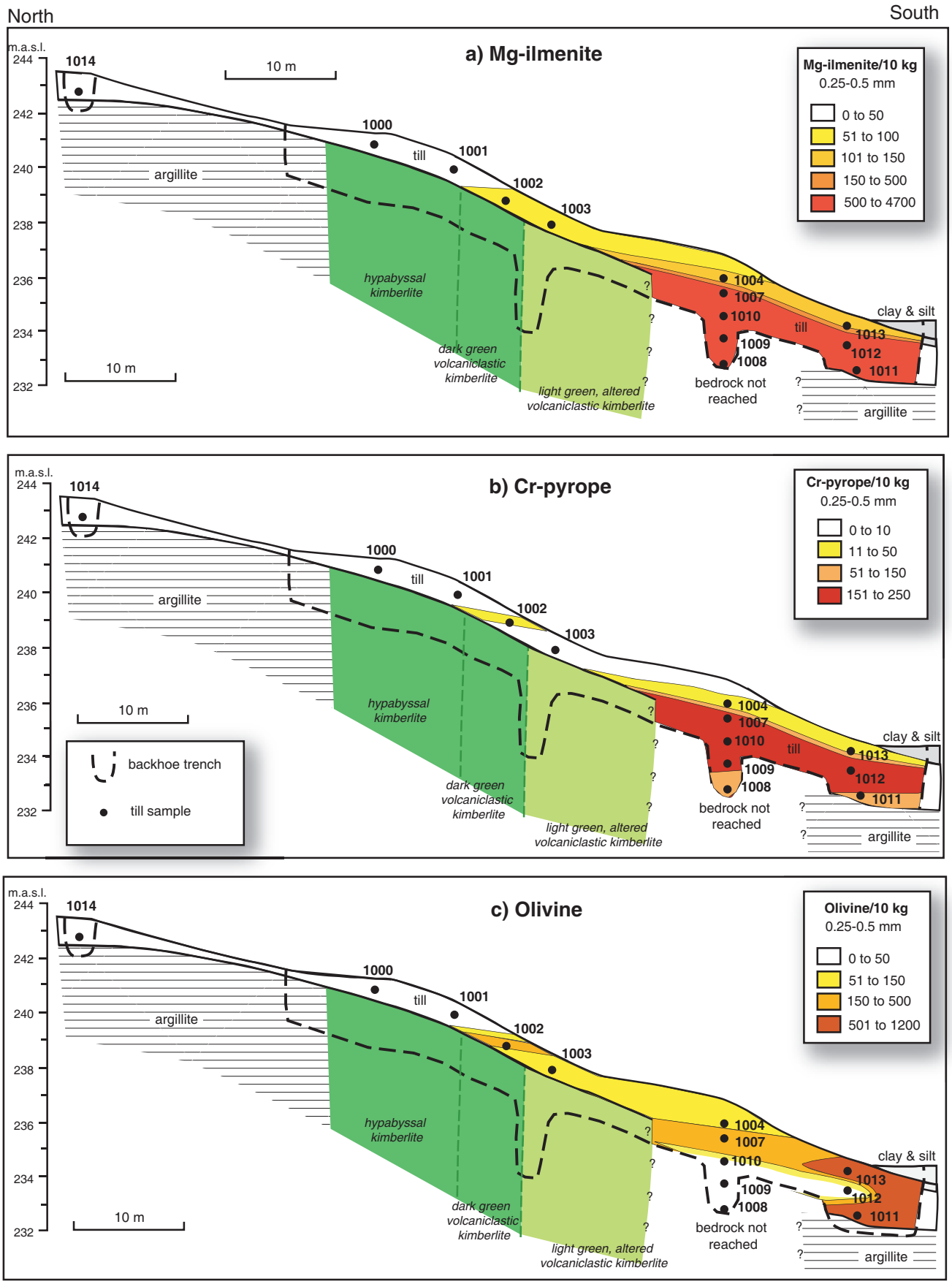

Figure 10. Schematic north-south section across the Triple B kimberlite showing abundance of: **a)** Mg-ilmenite; **b)** pyrope; and **c)** olivine.

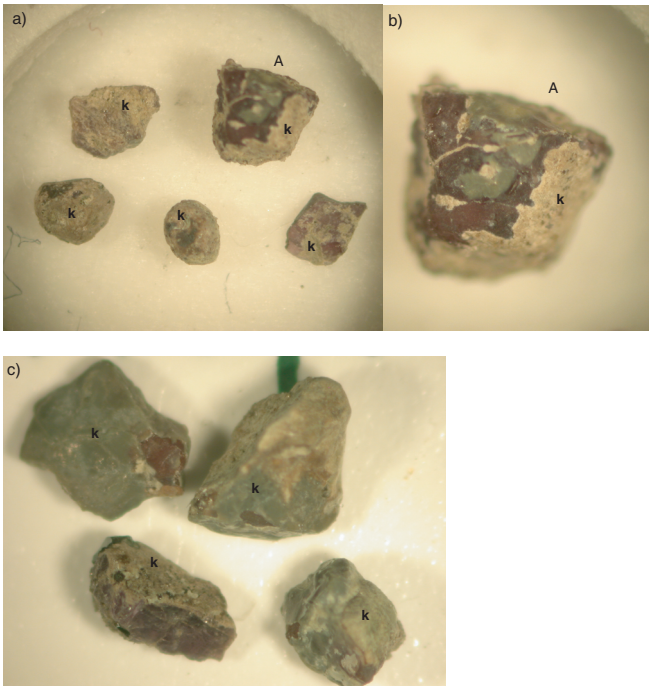

Figure 11. Colour photographs of Cr-pyrope grains from the 1-2 mm fraction of weathered Triple B kimberlite and till collected 23 m down-ice. Grey to light brown kelyphite coatings indicated by the letter **k**: **a)** kimberlite sample MPB-02-1006; **b**) enlargement of grain (A); **c)** till sample MPB-02-1009.

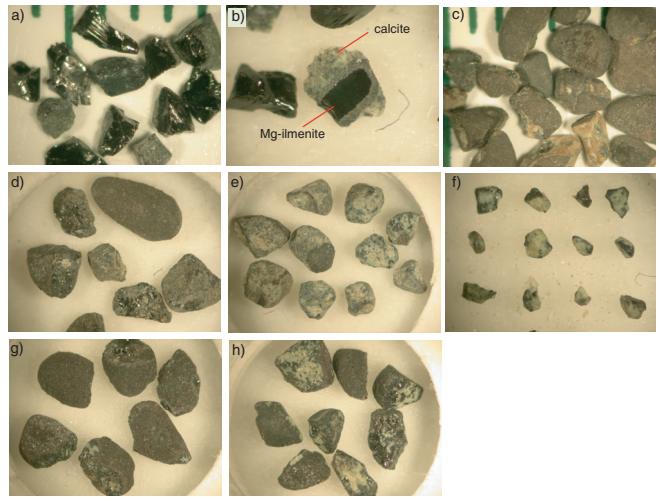

Figure 12. Colour photographs of Mg-ilmenite grains from weathered Triple B kimberlite and till samples collected down-ice. Mg-ilmenite grains are coated with grey-green serpentine and white calcite: **a)** angular shards in 1-2 mm fraction of mechanically crushed kimberlite sample KIA-02-TB; **b)** close up of grains from the 1-2 mm fraction of mechanically crushed kimberlite sample KIA-02-TB; **c)** subrounded grains from the 1-2 mm fraction of kimberlite sample MPB-02-1006; **d)** subrounded to subangular grains from the 1-2 mm fraction of till sample MPB-02-1007; **e)** subangular to subrounded grains from the 1-2 mm fraction of till sample MPB-02-1008; **f)** angular grains from the 0.25-0.5 mm fraction of till sample MPB-02-1008; **g)** and **h)** subangular to subrounded grains from the 1-2 mm fraction of till sample MPB-02-1010.

(sample MPB-SD-035) and 18 in till samples taken down-ice from the Triple B kimberlite. The coarse perovskite grains of the Triple B kimberlite can be used as an additional indicator mineral and their occurrence in till samples down-ice from Triple B is a further indication that the till indeed contains material from the Triple B kimberlite. Perovskite is also an important mineral for U/Pb age dating of kimberlites (e.g. Heaman and Kjarsgaard, 2000) and kimberlite boulders (Kjarsgaard et al., 2004).

PYROPE AND MG-ILMENITE SURFACE TEXTURES

Photographs of Cr-pyrope and Mg-ilmenite grains are included here to show examples of grain shape and surface features from the Triple B kimberlite and till within 20 m of its source. Kelyphite coatings are abundant on Cr-pyrope (Fig. 11) grains in weathered kimberlite and till. Calcite and serpentine overgrowths are common on Mg-ilmenite grains from the kimberlite and till samples between 10 and 20 m south of the kimberlite (Fig. 12).

KIMBERLITE INDICATOR MINERAL CHEMISTRY

Mg-Ilmenite

Seed kimberlite

The compositional range of Mg-ilmenite in the Seed kimberlite is characterized by a broad scatter from 8.5 to 18 wt.% MgO and from 0.2 to 4.5 wt.% Cr_2O_3, with few grains containing MgO <10 wt.% (Fig. 13a). In contrast to other kimberlites in the region, there is no discernible trend in the Cr_2O_3 versus MgO distribution. The compositional range of the Mg-ilmenite data reported in this study overlaps that of Mg-ilmenite compositions reported for the Seed kimberlite sampled from drill core (Sage, 2000; Fig. 13a), but extends to higher MgO concentrations.

Approximately 69% of the Mg-ilmenite grains found in the till samples around the Seed kimberlite contain less MgO (<10 wt.%) and Cr_2O_3 (<0.5 wt.%) than those from the Seed kimberlite. Only Mg-ilmenite compositions from till samples MPB-SD-010, immediately overlying the Seed kimberlite and sample SD-02-020 50 m southeast of the kimberlite, fully overlap with the compositional range of the Seed kimberlite (Fig. 13b). Mg-ilmenite from other till samples define a compositional range that is characterized by: 1) a group of low MgO-low Cr_2O_3 grains (6-8.5 wt.% MgO, 0.2-0.7 wt.% Cr_2O_3) and 2) a second group of higher MgO/very low Cr_2O_3 grains (9-12.5 wt.% MgO, <0.5 wt.% Cr_2O_3) divided by a small hiatus at ca 8.5 to 9 wt.% MgO with a few outliers at higher Cr_2O_3 (>0.8-4 wt.% Cr_2O_3) at low and medium MgO values (Fig 13b).

Triple B kimberlite

The composition of Mg-ilmenite from the Triple B kimberlite mimics the MgO versus Cr_2O_3 distribution of the Seed kimberlite with some additional grains towards slightly lower MgO and Cr_2O_3 contents (Fig. 13d). Mg-ilmenite compositions in the three Triple B kimberlite samples show little difference from each other, whereas Mg-ilmenite from the adjacent kimberlite dyke (sample MPB-SD-035) exhibits a more restricted range in MgO from 11 to 15 wt.% (Fig. 13e).

Most Mg-ilmenite in till samples collected overlying and down-ice from the Triple B kimberlite and dyke overlap in

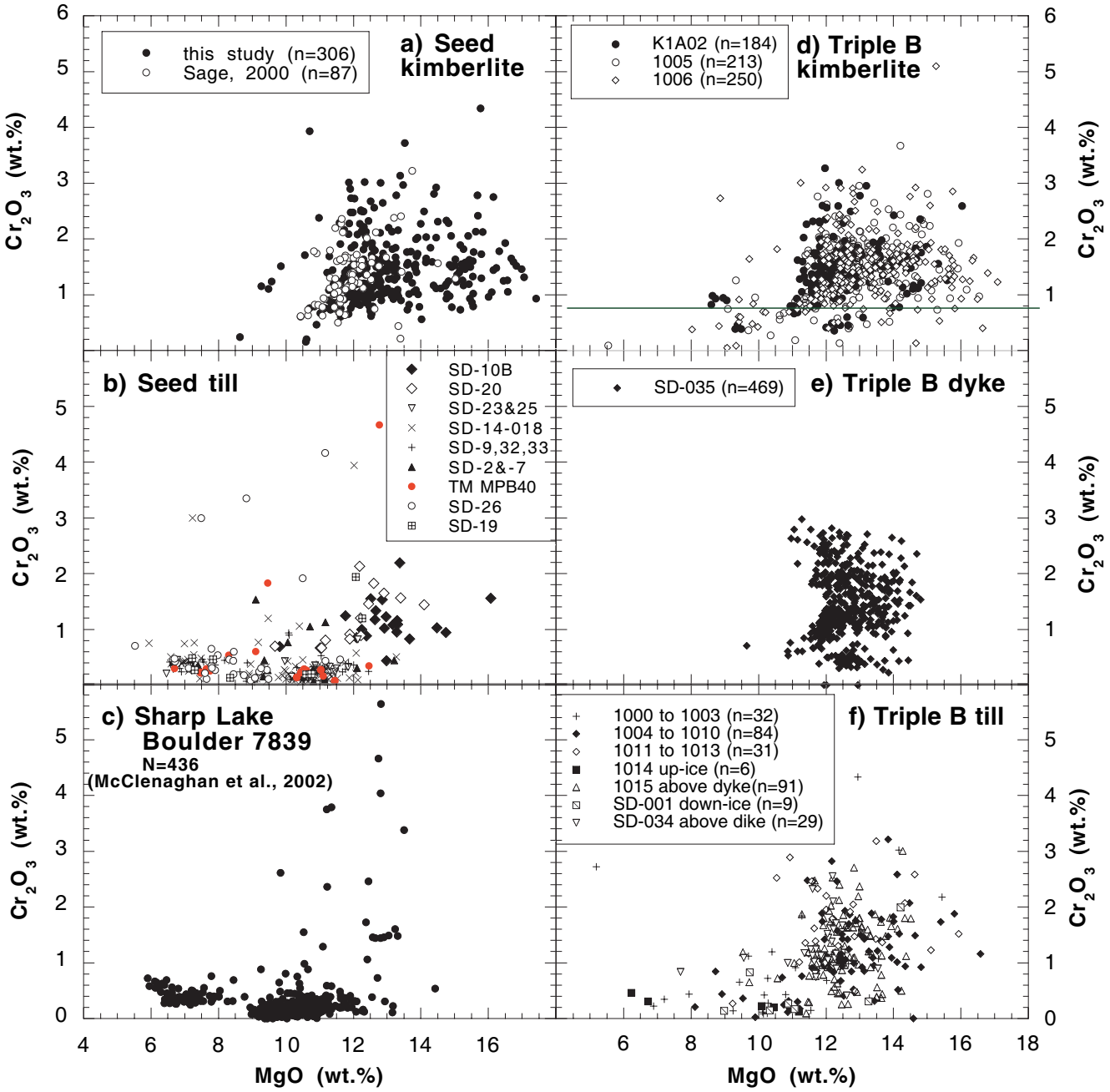

Figure 13. Bivariate plots of MgO versus Cr_2O_3 in Mg-ilmenite from: **a)** Seed kimberlite (with data from Sage, 2000); **b)** Seed till (subdivided by sample locations/ trenches); **c)** a boulder from the Sharp Lake pit (sample 97MPB7839, data from McClenaghan et al., 2002b); **d)** Triple B kimberlite body; **e)** Triple B dyke; and **f)** Triple B till (subdivided by sample locations/trenches).

composition with those of the kimberlite (Fig. 13f). However, a few grains from samples MPB-02-1014 (up-ice from Triple B), MPB-02-1000 to MPB-02-1004 (immediately overlying the kimberlite) and MPB-SD-001 (100 m southwest) contain less MgO and more Cr_2O_3 and are compositionally different from the Triple B kimberlite. These grains have the same compositional range as most Mg-ilmenite south of the Seed kimberlite (Fig. 13b).

Garnet

Seed kimberlite

Garnets from the Seed kimberlite are mainly purple, lherzolitic pyrope garnet with Cr_2O_3 contents ranging from 1.5 to <10 wt.% (Fig. 14a). Most orange garnets recovered from the kimberlite, picked as potential eclogitic garnets, are almandine-spessartine garnet (26–36 wt.% FeO_{tot}, mainly with <3 wt.% MnO, and 2.77–8.58 wt.% MgO, except for three grains with 11–14% wt.% MgO). These garnet grains are interpreted to be derived from crustal xenoliths entrained in the kimberlite. Megacryst garnets are scarce (only 3) in the Seed kimberlite and eclogitic garnets are absent. A few high Ti/high Cr-pyropes recovered are considered to be from sheared and/or metasomatized lherzolite xenoliths. No subcalcic harzburgitic garnets were found. A larger garnet data set for Seed kimberlite drill core (Sage, 2000) confirms the absence of eclogitic and subcalcic harzburgitic garnets but shows an additional population of unusual, high Ca/high

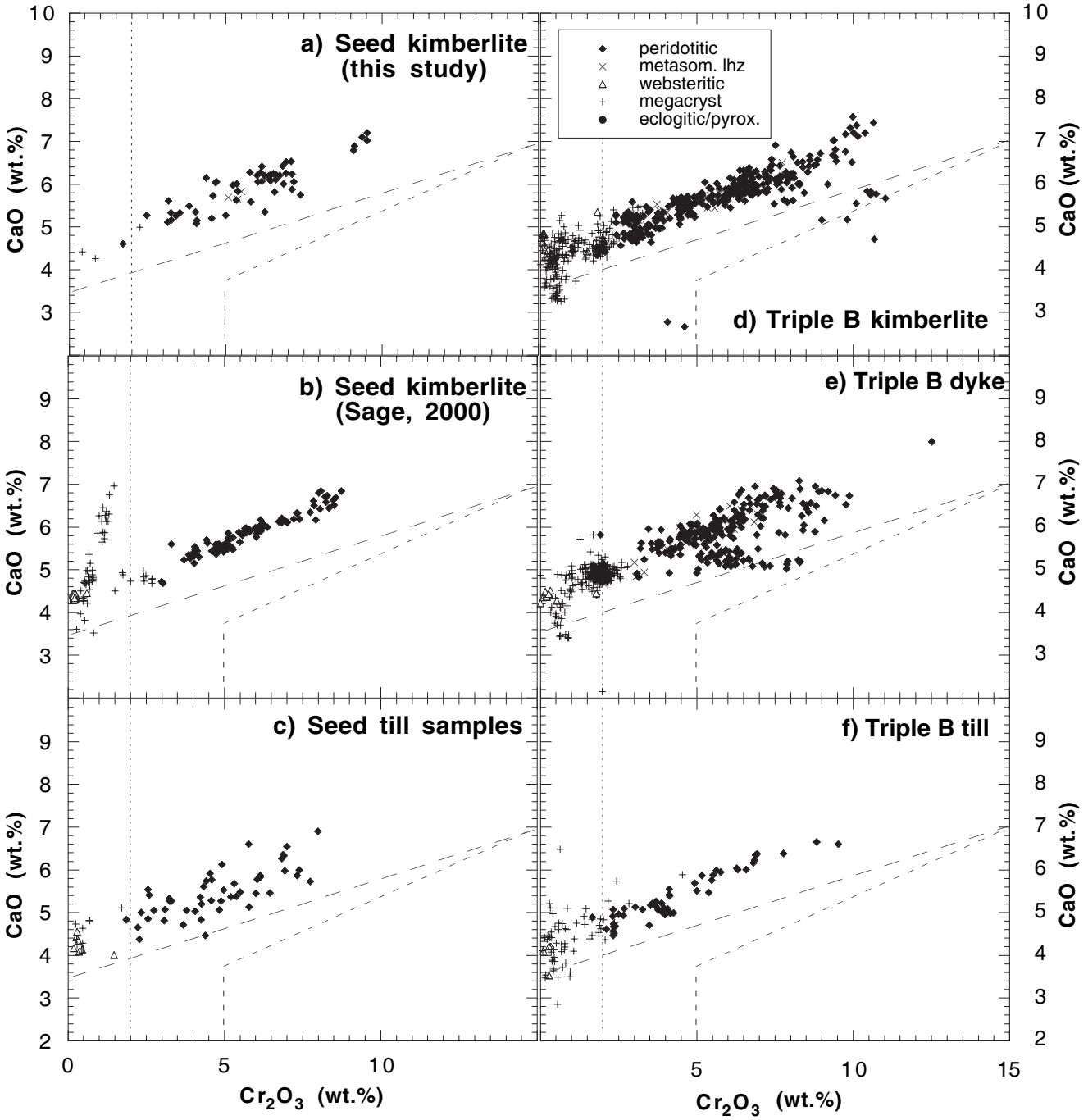

Figure 14. Bivariate plots of CaO versus Cr_2O_3 in garnet from: **a)** Seed kimberlite (this study); **b)** Seed kimberlite (Sage, 2000); **c)** Seed till samples; **d)** Triple B kimberlite body; **e)** Triple B dyke (sample MPB-SD-035); and **f)** Triple B till samples. The diagonal dashed line is the 85% line defined by Gurney (1984) and the dashed field below is the field of subcalcic garnet (Sobolev, 1977).

Ti/low Cr pyropes, which have much higher CaO and TiO_2 content than common megacrysts (Fig. 14b). Pyrope with compositions similar to this unusual group is known only from the Bucke kimberlite, where they are slightly more Cr-rich (Sage, 2000). The origin of these garnets remains unresolved. Sage (2000), based on data from Kopylova et al. (1999), speculates that the unusual pyropes might be from garnet-spinel lherzolites. If so, these lherzolites would have undergone metasomatism in order to account for their relatively high TiO_2 (>1-2.5 wt.%) and CaO (>5.5 wt.%) content. Alternately, they may be of websteritic paragenesis.

Garnet is rare in the till samples collected around and down-ice from the Seed kimberlite. Pyrope found in till samples is predominantly lherzolitic, containing up to 8 wt.% Cr_2O_3, with only a few grains of websteritic and megacryst origin (Fig 14c). Garnet chemistry cannot be used to determine if the grains are derived from the Seed kimberlite or from other sources.

Triple B kimberlite

Garnet in Triple B kimberlite can be grouped into four different lithologies (Fig. 14d): 1) peridotitic Cr-pyrope with up

to 13 wt.% Cr_2O_3; 2) abundant megacryst garnet containing approximately 0.5 wt.% Cr_2O_3 and 2 wt.% Cr_2O_3; 3) a few high Ti-high Cr garnets from sheared/metasomatized lherzolite; and 4) a few low Cr websteritic garnets. Some of the Cr-rich harzburgitic/dunitic garnets plot below Gurney's (1984) 85% line and into Sobolev's (1977) field for subcalcic harzburgitic garnets. One potentially eclogitic garnet (FeO_{tot}< 22 wt.%, MgO> 5 wt.%) was found among several orange crustal almandine-spessartine garnets recovered from the kimberlite samples.

Garnet compositions in the Triple B kimberlite dyke (sample MPB-SD-035) show some slight variations from those in the main body (Fig. 14e); the megacryst garnets are mostly Cr-rich, i.e. they belong to the second population of megacrysts identified in the main kimberlite body. The peridotitic garnets contain an additional population that deviates from the lherzolite trend (parallel to the 85% line) and straddles the 85% line. However, subcalcic harzburgitic garnets similar to those found in the other three Triple B kimberlite samples are absent.

Triple B till samples (Fig. 14f) contain peridotitic and megacryst garnet. The megacryst garnets are predominantly Cr-poor and are likely derived from the main Triple B body instead of from the dyke, having compositions that plot above the 85% line.

Cr-Diopside

Seed kimberlite

Cr-diopside recovered from the Seed kimberlite sample MPB-SD-013 is fairly high in Cr_2O_3 (0.7-2.9 wt.%) with a range of Mg numbers (100 Mg/(Mg+Fe^{2+})) from 86 to 93, encompassing both peridotitic and less ultramafic lithologies (Fig. 15a). No (low Cr-) megacrysts diopsides were recovered. No Cr-diopside data from other studies of the Seed kimberlite are available for comparison.

Most Cr-diopside compositions in till samples near the Seed kimberlite cluster around 1 wt.% Cr_2O_3 with Mg numbers of between 84 and 87 (box in Fig. 15a). Cr-diopside of this particular compositional range is absent in the Seed kimberlite, but is well documented in till from the greater Kirkland Lake and Lake Timiskaming regions, and is likely derived from regional ultramafic rocks (McClenaghan et al., 1999, 2001, 2002a). Some till samples (MPB-SD-002, -009, -010, -026, -032 and -033) contain Cr-diopside of peridotitic compositions (high Mg numbers of >88 and >0.5 wt.% Cr_2O_3) that overlap or even exceed those of the Seed kimberlite. The latter, found in samples MPB-SD-026 and -033, might be an indication of an additional kimberlitic source of Cr-diopside in the till samples.

Triple B kimberlite

Cr-diopside from the Triple B kimberlite occupies the same compositional range as that from the Seed kimberlite, ranging from 0.2 to 3.4 wt.% Cr_2O_3 with Mg numbers between 87 and 93 (Fig. 15b). Cr-diopside compositions from till around the Triple B kimberlite (Fig. 15b) plot in the compositional field of regional ultramafic rocks outlined in Figure 15b and barely overlaps with the Cr-diopside recovered from the Triple B kimberlite.

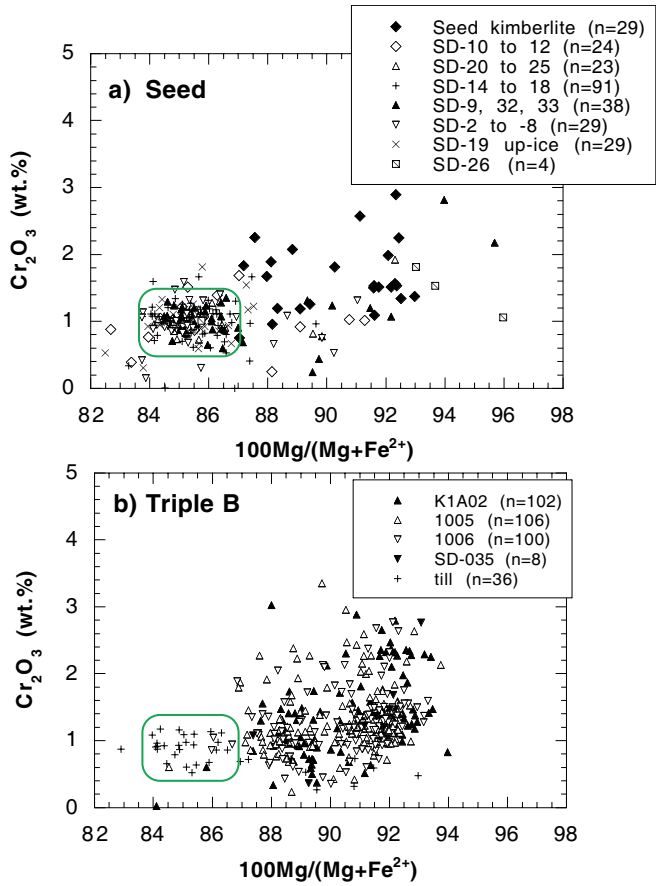

Figure 15. Bivariate plots of Cr_2O_3 versus Mg number (100Fe/(Fe+Mg)) in Cr-diopside from the: **a)** Seed kimberlite and till samples; **b)** Triple B kimberlite, dyke and till samples. The green box indicates the compositional field of Cr-diopside from regional till samples from the Kirkland Lake and Lake Timiskaming areas that are interpreted to be derived from regional ultramafic rocks.

Chromite

Seed kimberlite

Chromite grains from the Seed kimberlite plot just below the diamond-inclusion field (Fig. 16a). Sage (2000) recovered 46 chromite grains from a large drill core sample of hypabyssal Seed kimberlite that scatter towards lower MgO at equal Cr_2O_3 compared with data from this study (Fig. 16a). The combined pattern from both data sets is similar to chromite compositions from other Lake Timiskaming kimberlites (Sage, 1996, 2000; McClenaghan et al., 1999, 2002a, 2003).

Compositions of chromite in till around the Seed kimberlite range from just below the diamond inclusion field to very MgO-poor (ferro-)chromites with about 50 wt.% Cr_2O_3 as well as to MgO-rich/Cr-poor Cr-spinel compositions (Fig. 16a). Ferro-chromite with <6 wt.% MgO found in some of these till samples has not been reported in any of the kimberlites from the Lake Timiskaming field and the grains are most likely from regional ultramafic rocks or are products of metasomatic reactions.

Triple B kimberlite

Chromite compositions in the Triple B kimberlite show more scatter towards Cr- and MgO-poor compositions (Cr-spinel)

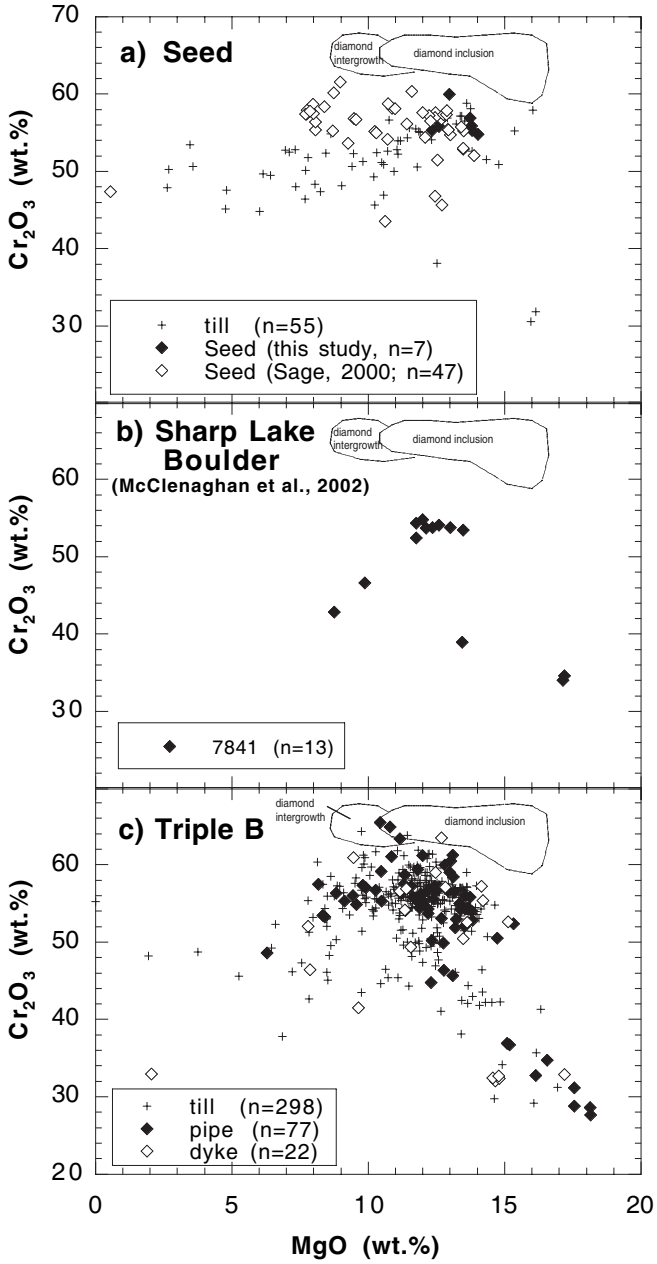

Figure 16. Bivariate plots of MgO versus Cr_2O_3 in chromite from the: **a)** Seed kimberlite (with data from Sage, 2000) and till samples; **b)** Sharp Lake pit boulder (97MPB7841; data from McClenaghan et al., 2002b); **c)** Triple B kimberlite, dyke and till. Diamond inclusion and intergrowth fields are from Fipke et al. (1995)

than those from the Seed kimberlite. Several Cr-rich (magnesiochromite) grains have compositions that plot within the diamond-inclusion or diamond-intergrowth fields (Fig. 16c). Chromite compositions in the Triple B dyke overlap in composition with those of the main kimberlite body (Fig. 16c). Six Ti-rich chromian and aluminous magnesioferrite grains containing about 16 wt.% MgO and 23 wt.% TiO_2 were recovered from sample K1A02-TB. They plot outside the boundaries of Figure 16c because of their very low Cr_2O_3 content (<5.4 wt.%) and have no equivalent in other kimberlite or till samples. Chromite compositions in till samples around the Triple B kimberlite are similar to those in the Triple B kimberlite, with the exception of a few ferrochromite grains and several chromites containing between 38 and 48% Cr_2O_3 (Fig. 16c), which might be from regional ultramafic rocks.

Olivine

Seed kimberlite

No fresh olivine was recovered from the Seed kimberlite in this study; Sage (2000) analyzed only one grain in his study of Seed drill core samples (see previous sections on kimberlite geology and kimberlite indicator mineral abundances). Fresh olivine grains were not recovered from till samples around the Seed kimberlite, but were found in sand sample MPB-SD-026 from the Caldwell gravel pit (Fig. 17a). These grains have Mg-numbers (Fo contents) ranging from 86 to 94.5, and NiO contents from 0.20 to 0.45 wt.% NiO. Compositions with Fo >90 are typical of peridotitic mantle olivine. The grains with Fo 86-89 probably represent kimberlite phenocrystal olivine, or alternately might be derived from olivine-bearing regional ultramafic rocks.

Triple B kimberlite

Dyke sample MPB-SD-035 did not contain any olivine. Olivine from the three Triple B kimberlite samples has Fo contents ranging from 83 to 93 (Fig. 17b) with a compositional break at about Fo 89.5. Olivine with Fo <89.5 and NiO <0.25 wt.% is considered to be potential kimberlite phe-

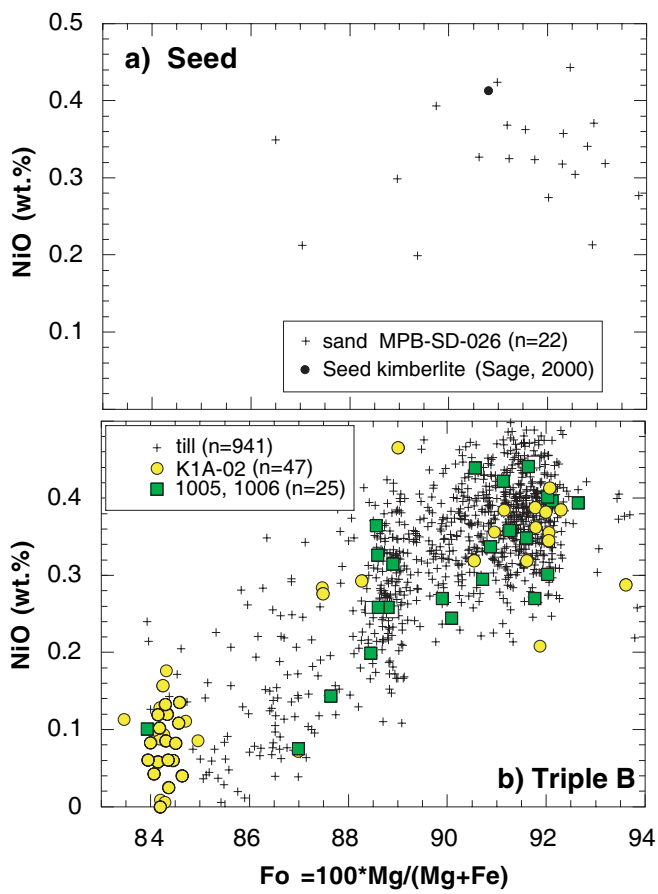

Figure 17. Bivariate plots of NiO versus Fo (100Fe/(Fe+Mg)) in olivine from the: **a)** Seed kimberlite (Sage, 2000) and sand sample MPB-SD-026; and **b)** Triple B kimberlite and till samples.

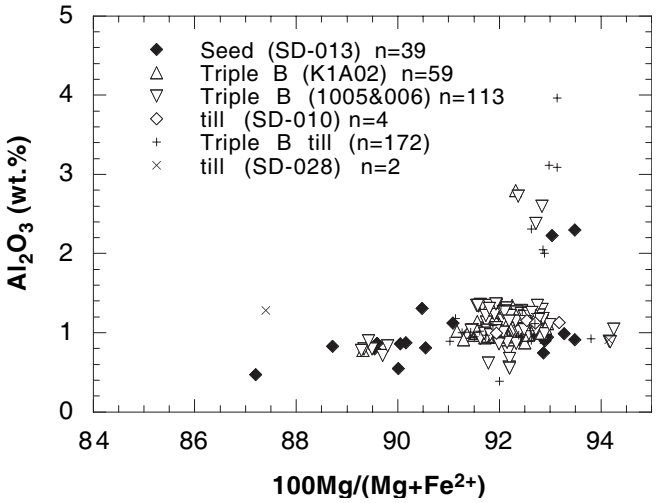

Figure 18. Plot of Al_2O_3 versus Mg number (100Fe/(Fe+Mg)) in enstatite from the Seed and Triple B kimberlites, and till samples.

nocrysts, whereas olivines with Fo >89.5 are interpreted to be derived from dissaggregated peridotite xenoliths. Abundant olivine grains occur in till samples MPB-02-1002, -1007, -1011, and -1013 and they are similar in compositional range to those from the Triple B kimberlite. Most of these olivine grains have Fo >89.5 and >0.22 wt.% NiO.

Enstatite

Seed kimberlite

Although not systematically picked and analysed, a few visually identified enstatite grains from the Seed kimberlite were analyzed to determine their compositional range. They contain 0.5 to 4.0 wt.% Al_2O_3 and have Mg numbers ranging from 89 to 93.5, which is consistent with a peridotitic origin (Fig. 18).

Triple B kimberlite

Enstatite grains recovered from Triple B kimberlite samples MPB-02-1005 and K1A02-TB were picked and analysed because they were thought to be olivine. The composition of the grains indicates a high proportion of orthopyroxene-bearing peridotite in the Triple B kimberlite, which overlaps in composition with that found in the Seed kimberlite (Fig. 18).

PEBBLE LITHOLOGY

Seed kimberlite

Till samples around the Seed kimberlite contain mostly locally derived Huronian metasedimentary (argillite) clasts

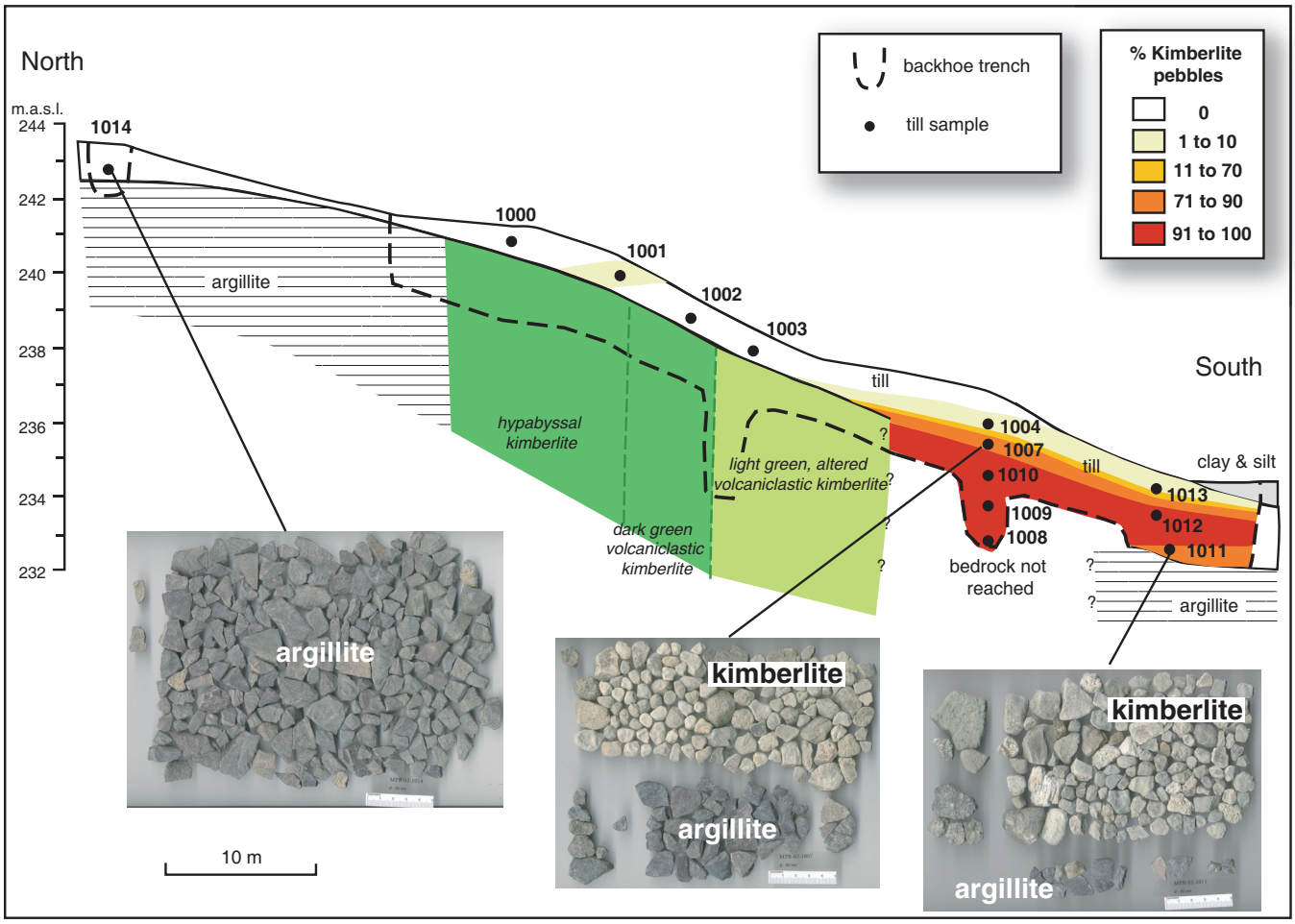

Figure 19. Schematic north-south section across the Triple B kimberlite showing the abundance (frequency %) of kimberlite clasts in the 0.8 to 5 cm fraction of till.

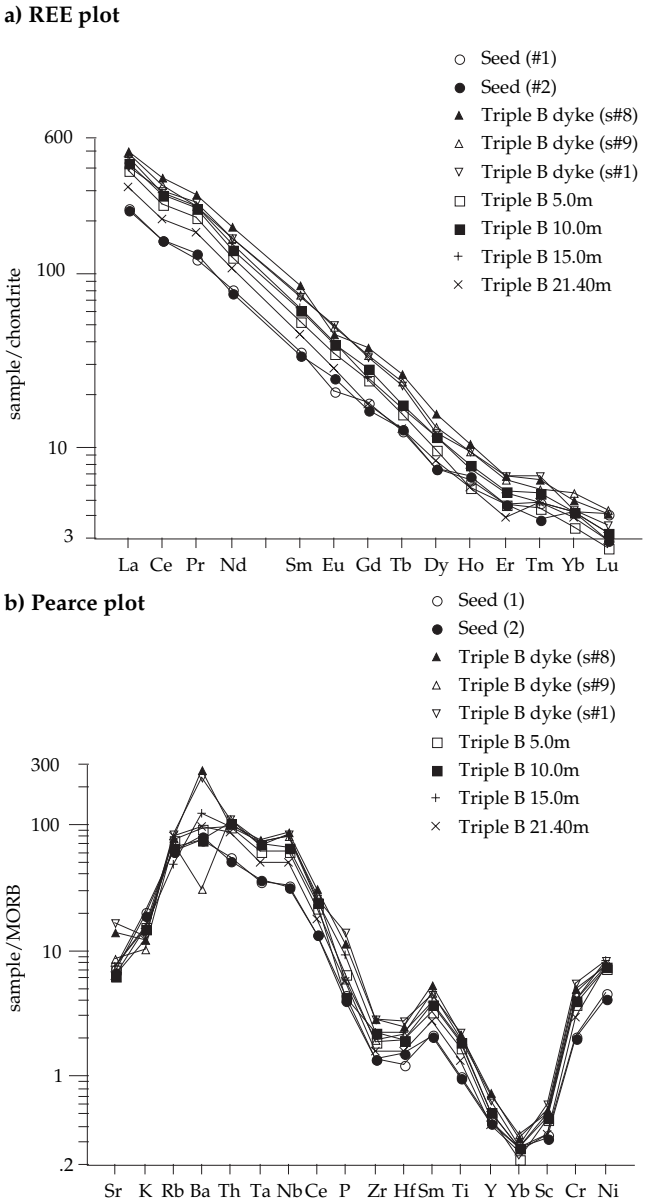

Figure 20. a) Chondrite normalized REE plot, and **b)** Pearce plot for: two Seed kimberlite samples; three samples of the Triple B kimberlite dyke; and four samples from the Triple B kimberlite pipe.

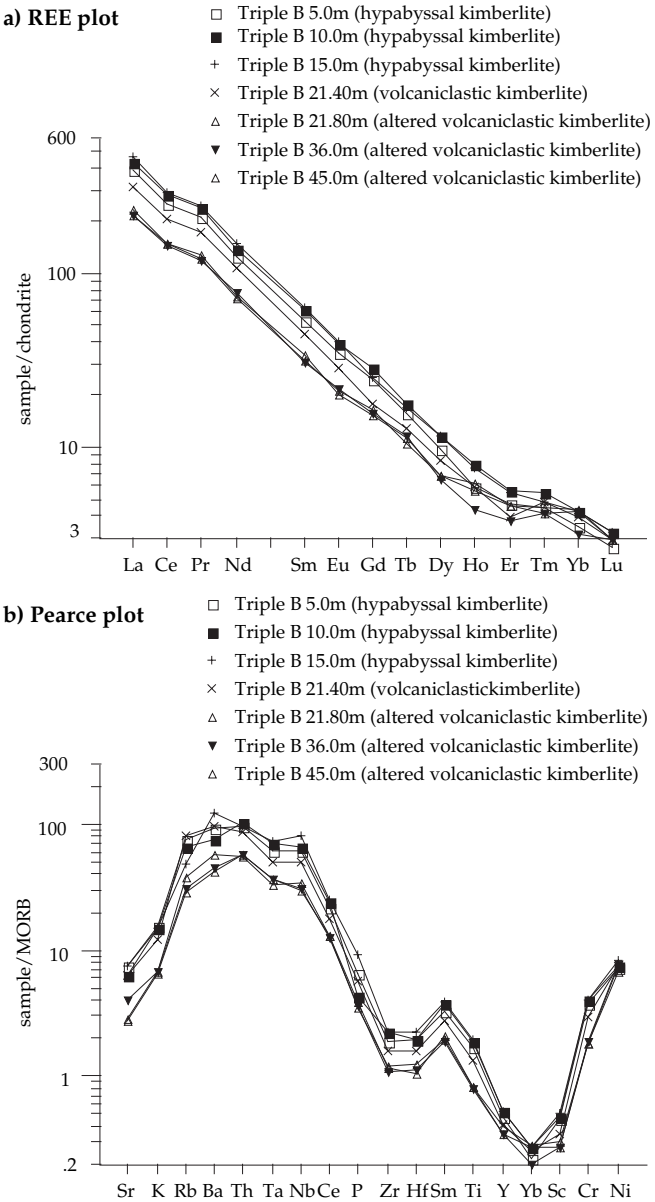

Figure 21. a) Chondrite normalized REE plot, and **b)** Pearce plot for four Triple B kimberlite samples and three till samples down-ice.

(46–86%) from the Lorraine Formation and carbonate clasts (0.5–36.5%) derived from outcrops of Paleozoic platform carbonate rocks 5 km to the northeast of the Seed kimberlite (Fig. 2) (Appendix B). Paleozoic carbonate clast content is much greater in fresh, unweathered till samples (15–36.5 %) as compared to shallow (<1.5 m depth) till samples (0.5 and 7.5 %) in which most carbonate clasts have been destroyed by postglacial weathering and oxidation. Kimberlite fragments were found only in till sample MPB-SD-032, 100 m down-ice (southeast) of the Seed kimberlite.

Triple B kimberlite

Till samples up-ice and overlying the Triple B kimberlite contain mostly local Huronian metasedimentary (argillite) rocks (75–99%) of the Lorraine Formation, and a few Paleozoic carbonate clasts (0–3.5%; Fig. 19). The Paleozoic carbonate content is likely much lower in these till samples, as compared to the Seed kimberlite, because most samples were collected near surface (<1 m depth) and the carbonate clasts have been destroyed by postglacial weathering. Till samples down-ice of the Triple B are dominated by kimberlite pebbles (72–100%) (Fig. 19).

KIMBERLITE GEOCHEMISTRY

The REE geochemistry of the Seed kimberlite, Triple B kimberlite dyke, and Triple B kimberlite is presented in Figure 20a, and a multi-element spider (Pearce plot) diagram for these samples is presented in Figure 20b. The high LREE enrichment and steep REE profile, as well as high concentrations of Ba, Th, Ta, Nb, P, Cr, and Ni is consistent with the known geochemical signature of Group I kimberlites (e.g. Mitchell, 1986, 1995). The volcaniclastic (diatreme) Seed kimberlite samples have slightly lower concentrations, con-

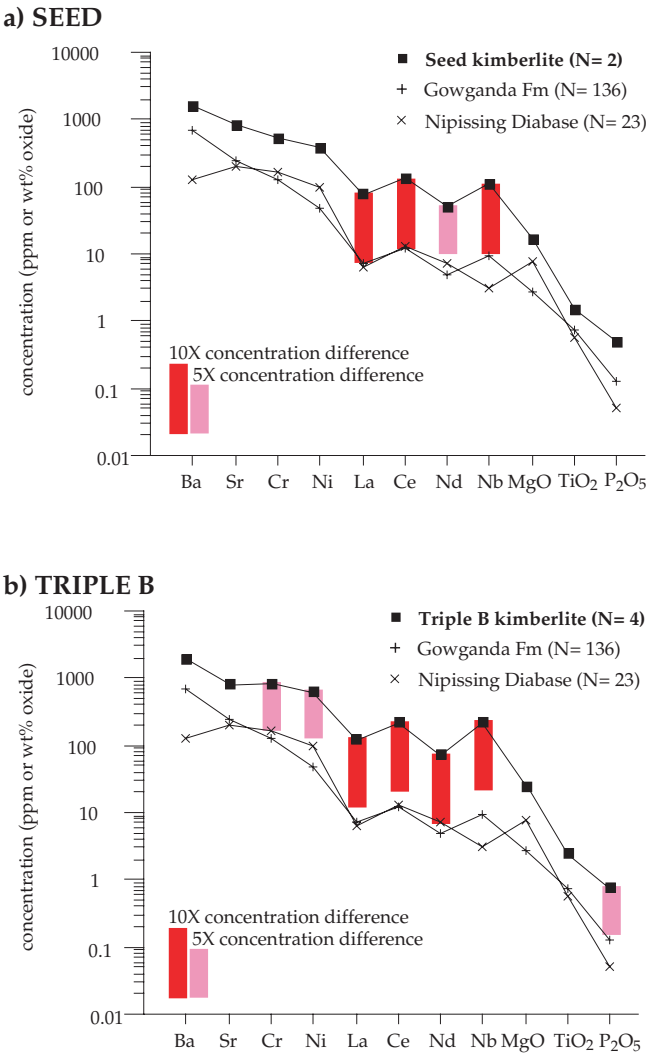

Figure 22. Comparison of selected trace and major element average concentrations in local country rock versus: **a)** the Seed kimberlite; and **b)** the Triple B kimberlite. Elements for which concentrations are at least 5 to 10 greater in the kimberlites as compared to the country rock are highlighted in red or pink as potential pathfinder elements for till geochemistry. Gowganda Fm data from Young and Nisbett (1999); Nipissing diabase data from Lightfoot et al. (1993).

sistent with the observation that these samples are contaminated by >15 modal% crustal xenoliths. Similarly, the Triple B volcaniclastic (diatreme) kimberlite sample (at 21.40 m) has slightly lower concentrations compared to the weakly crustally contaminated Triple B hypabyssal kimberlite samples (at 5.0, 10.0, and 15.0 m) as seen in Figure 21a and b. The highly altered Triple B volcaniclastic (diatreme) kimberlite samples contain even lower concentration levels (Fig. 21a,b). Two samples of Triple B kimberlite dyke are enriched in Ba and Sr (Fig. 20b) compared to the main body of the Triple B kimberlite and the Seed kimberlite.

The major and trace element geochemical signature of the Seed and Triple B kimberlites is compared to the bedrock geochemical signature of the Nipissing diabase and Gowganda Formation (the local host rocks) in Figure 22. Note that the Gowganda data set incorporates analyses of the Firstbrook Member of the Gowganda Formation. For the Seed kimberlite, the concentration of La, Ce, and Nb is 10 times higher and Nd is 5 times higher, as compared to the host rocks. For the Triple B kimberlite La, Ce, Nd, and Nb are 10 times higher and Cr, Ni, and P_2O_5 are 5 times higher as compared to the host rocks. These patterns indicate that La, Ce, Nd, Nb, Ni, Cr, and P_2O_5 are viable pathfinders elements for use in till geochemical exploration and glacial dispersal studies of kimberlites in the Timiskaming area.

TILL GEOCHEMISTRY

Geochemical data determined by $LiBO_2$ fusion as well as aqua regia are listed in Appendix E. Concentrations determined by aqua regia (Appendix E.4) are at or near the lower detection for most elements. Concentrations of Cu, Pb, and Zn, although above detection limit, are unremarkable and are similar to mean values for till in the Timiskaming region (McClenaghan et al., 2001). Ni values determined by aqua regia are, on average, 88% of the total values determined by $LiBO_2$ fusion (Appendix E.2). Aqua regia values for Ni are most similar to total values for the 0.063 to 0.25 mm fraction (95% of total values) and least similar for the 0.5 to 1.0 mm fraction (81% of total values). For this reason, only Ni values determined by $LiBO_2$ fusion will be discussed in this report.

Till samples up-ice (sample MPB-02-1014) and overlying the Triple B kimberlite (samples MPB-02-1000 to -1003) are considered to reflect background concentrations typical for local rocks other than kimberlite, as they do not contain significant numbers of indicator minerals (Table 1) or kimberlite pebbles (Appendix B). Till samples down-ice of the Triple B kimberlite have elevated concentrations of MgO, MnO, Ni, Ba, LREE, Ta, Nb, Sr, TiO_2, P_2O_5, Cr_2O_3, Th, U, and Co, elements that are typically enriched in kimberlite (Mitchell, 1986). The elements showing the most pronounced increases in concentration between background till samples versus kimberlite-rich till down-ice are: MgO (~2–25 wt.%), Ba (~500–1100 ppm), Nb (~10–300 ppm), Ni (~60–800 ppm), Ta (1.0–18 ppm), Cr_2O_3 (0.015–0.16 wt.%) and LREE. Most of these elements were predicted to be pathfinder elements for the Triple B kimberlite (Fig. 22). In contrast, SiO_2, Al_2O_3, Na_2O, and K_2O concentrations are significantly depleted in till down-ice.

Line plots of pyrope, Cr-diopside, Mg-ilmenite, chromite, and olivine abundances and element abundances in till samples along a north-south profile across the Triple B kimberlite are shown in Figure 23 and demonstrate the strong geochemical contrast between: a) till samples that contain few indicator minerals, and b) till samples that contain thousands of indicator minerals in both till near surface (<2 m depth) (samples MPB-02-1004, MPB-02-1013) and in till samples close to the till-bedrock interface (samples MPB-02-1008, MPB-02-1011). The plots for surface till and till near bedrock differ only in terms of samples between 8 and 20 m down-ice of the kimberlite, where the till thickens to between 5 and 10 m. Figure 23 also demonstrates the similarities and differences in geochemical responses of four different size fractions of the till matrix in background and anomalous till: 1) <0.063 mm (silt+clay); 2) 0.063 to 0.25 mm (fine sand); 3) 0.25 to 0.5 mm (medium sand); and 4) 0.5 to 2.0 mm (coarse to very coarse sand).

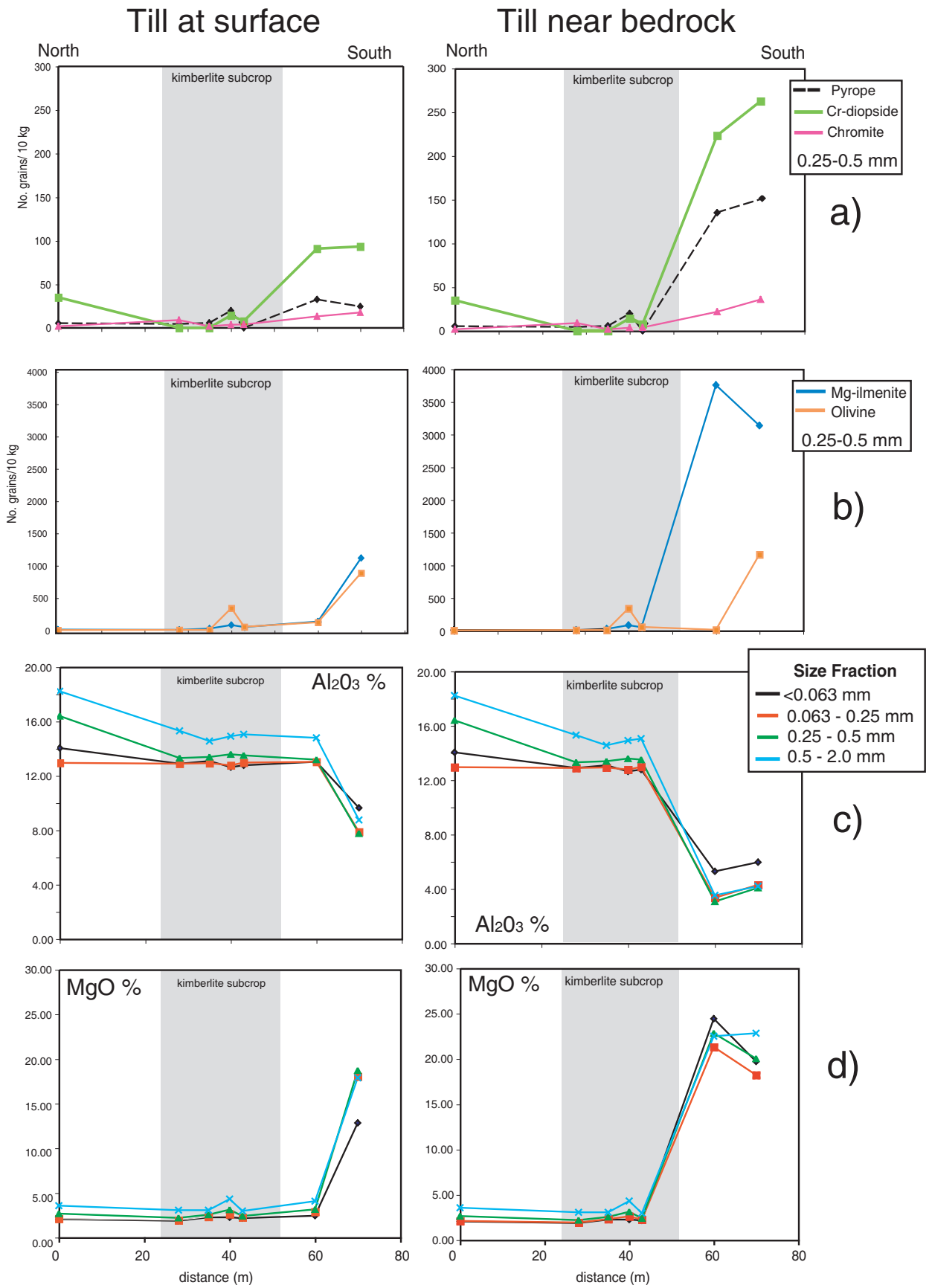

Figure 23. Comparison of indicator mineral abundances and Al_2O_3, MgO, Ni, Nb, Ba, Ce, and Ta concentrations, determined by $LiBO_2$ fusion, versus distance from the Triple B kimberlite for the <0.063, 0.063-0.25, 0.25-0.5 and 0.5 -2.0 mm fractions of till samples near surface and till samples at the till/bedrock interface.

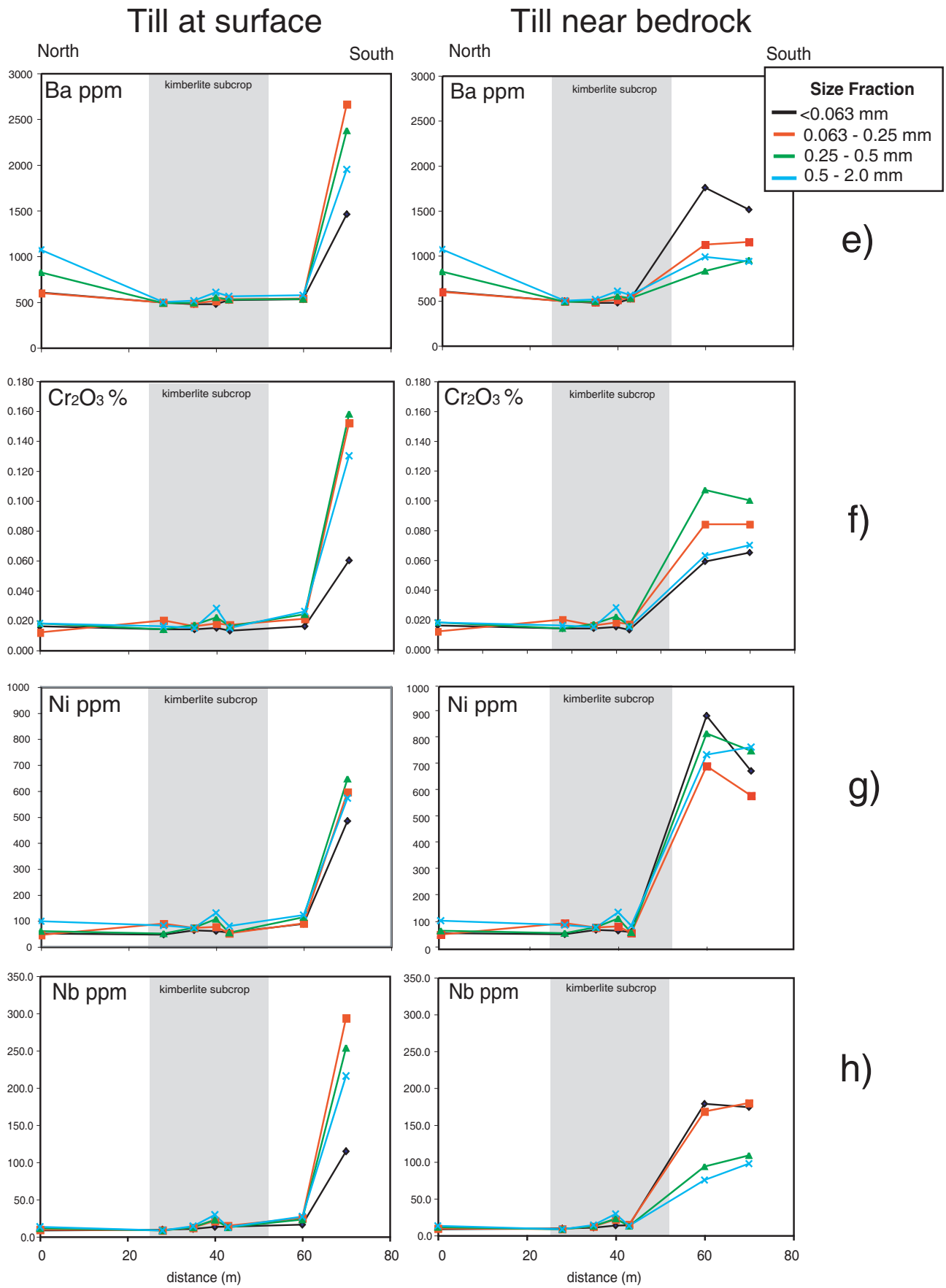

Figure 23. continued

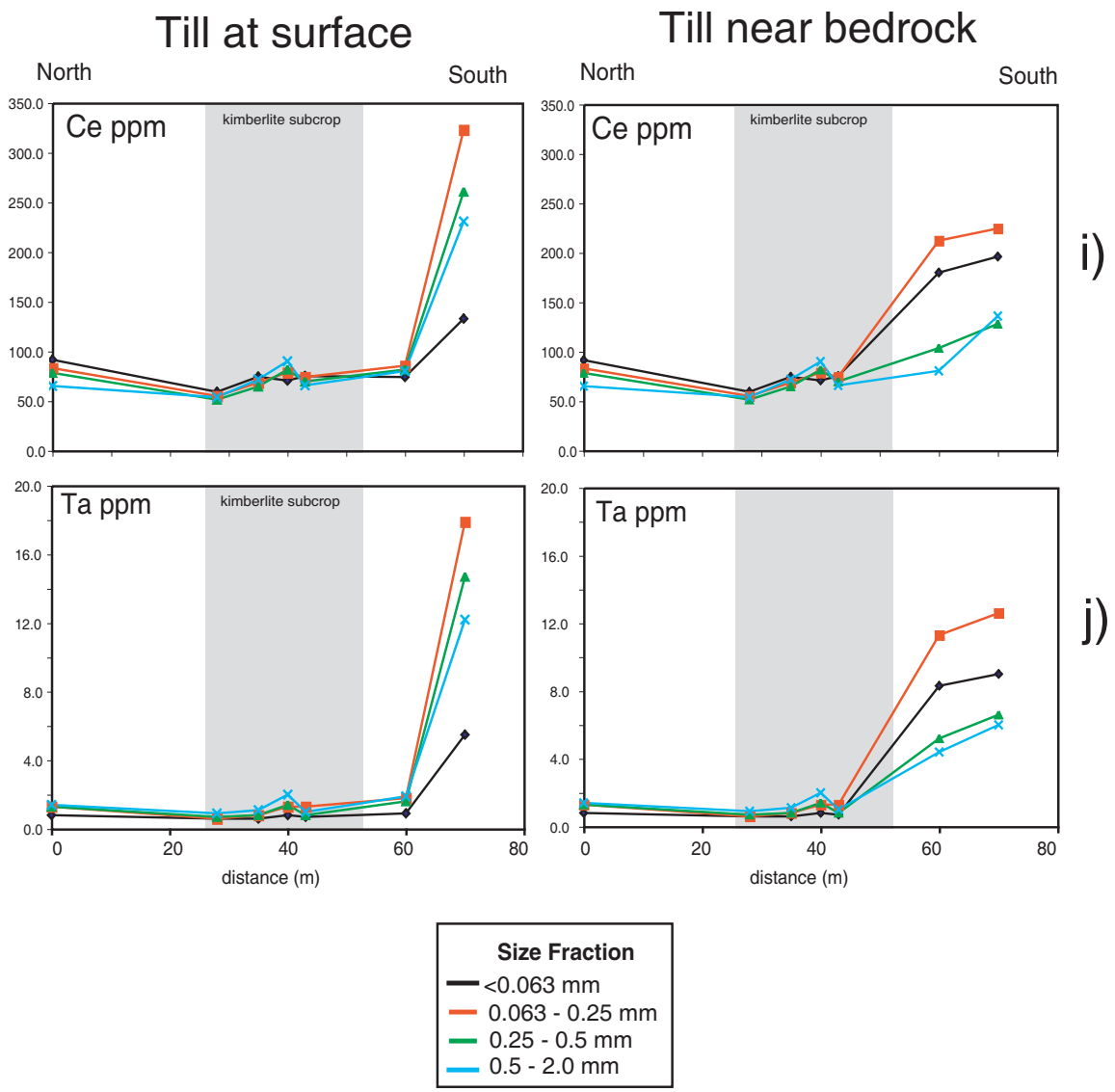

Figure 23. continued

Till at the Bedrock Interface

Comparison of element concentration patterns in the four size fractions of till (Fig. 23b-j) show the following characteristic changes from north (background) to south (till enriched in kimberlite debris) across the kimberlite:

1) similar patterns in all four size fractions of till are shown by Al_2O_3, MgO, and Ni concentrations. The strong decrease in Al_2O_3 concentration in till south of the kimberlite is due to the incorporation of kimberlitic material (depleted in Al_2O_3). In contrast, elevated values of MgO and Ni occur in all four size fractions immediately down-ice.
2) high values of Ba occur in both till samples down-ice and are most pronounced in the smallest size fraction (< 0.063mm).
3) the highest concentrations of Nb, Ta, and Ce occur in the two smallest size fractions (<0.063 mm, 0.063–0.25 mm) in the two till samples down-ice and with less pronounced increases in concentrations in the coarser fractions with distance down-ice from the kimberlite body.
4) the greatest increase of Cr_2O_3 concentration occurs in both mid-sized fractions (0.063–0.25 mm) and (0.25–0.5 mm) down-ice from the kimberlite.

Shallow Till (<2 m Depth)

Element concentration patterns in the four size fractions of shallow till samples are identical to those at depth for locations up-ice and overlying the kimberlite, where the overburden is thin (i.e. they exhibit low background levels of kimberlite specific elements and high levels of Al_2O_3). However, the levels remain low in the shallow till immediately down-ice from the kimberlite and only increase in the till sample farthest (20 m) down-ice. Element concentration patterns (Fig. 23b-j) show the following characteristic in this one sample 20 m to the south:

1) similar patterns in all four size fractions are shown by Al_2O_3, MgO, and Ni, with a strong depletion in Al_2O_3 concentration and elevated values of MgO and Ni.
2) highest concentrations in the two mid-sized fractions (0.063–0.25 mm and 0.25–0.5 mm) for Ba, Cr_2O_3, Ce, Nb, and Ta.

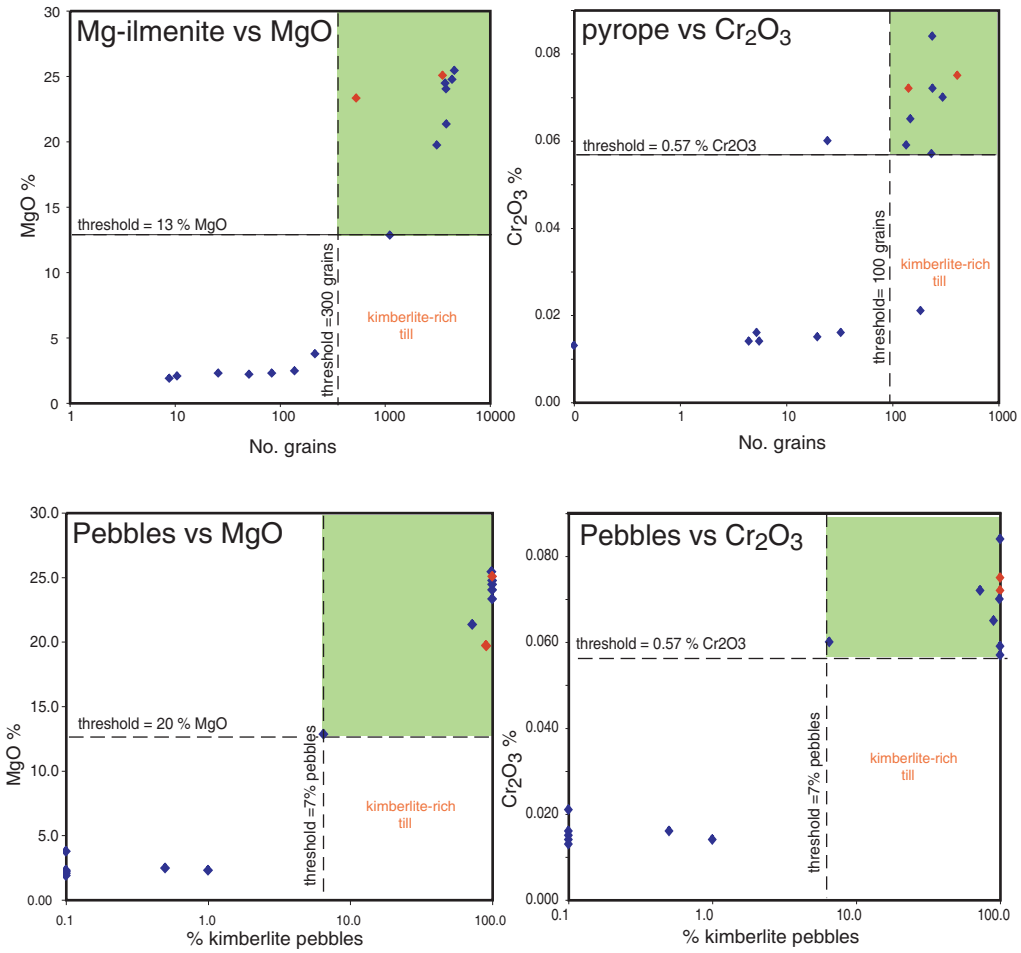

Figure 24. Bivariate plots of kimberlite pebble and indicator mineral abundance in the 0.25 to 0.5 mm nonferromagnetic heavy mineral fraction versus MgO and Cr_2O_3 concentration in the <0.063 mm fraction ($LiBO_2$ fusion) of the Triple B kimberlite (n=2; red diamond) and till (n=14; blue diamond).

3) of the four size fractions, the lowest concentrations of kimberlite specific elements are consistently in the <0.063 mm fraction, in contrast to till near the bedrock interface.

Comparison to Indicator Mineral and Pebble Counts

Indicator mineral counts and pebble counts provide indications of the amount of kimberlite debris in till samples around the Triple B kimberlite. Thus comparing indicator mineral and kimberlite pebble abundance to element concentrations in the till matrix will provide a crude indication of the number of indicator minerals present in till that display a kimberlite geochemical signature. Bivariate plots in Figure 24 provide a comparison between pyrope, Mg-ilmenite and kimberlite pebble abundances and the concentrations of MgO and Cr_2O_3 in the <0.063 mm fraction of till around the Triple B kimberlite. These plots are not meant to infer that the element abundances are directly proportional to the indicator mineral or kimberlite pebble abundances. Rather, the plots are meant to demonstrate merely the indicator mineral or pebble abundance levels at which the kimberlite pathfinder element concentrations are elevated for this particular kimberlite. The highest concentrations of the kimberlite pathfinder elements in till around the Triple B kimberlite, including MgO and Cr_2O_3 (Fig. 24), are found in till samples that contain approximately >300 grains of Mg-ilmenite, >92 grains of Cr-diopside, >100 grains of pyrope, and at least 7% kimberlite pebbles.

DISCUSSION

Seed Kimberlite

The relative abundance of indicator minerals in the Seed kimberlite is: Mg-ilmenite>>pyrope>Cr-diopside>chromite. The indicator mineral suite is characterized by abundant MgO- and Cr_2O_3-rich Mg-ilmenite, a few chromite grains that plot below the diamond-inclusion field, mostly lherzolitic Cr-pyrope garnet with very few megacryst garnets, and garnets from sheared lherzolite xenoliths. Cr-diopside is rare and belongs to a peridotitic paragenesis, as do enstatite grains that were recovered. No olivine was recovered from the Seed kimberlite due to almost complete alteration of olivine to serpentine. The Seed kimberlite can be characterized as having moderate indicator mineral abundance and is dominated by megacryst ilmenite with only a small proportion of Cr-pyrope, Cr-diopside, and chromite derived from dissaggregated lherzolitic mantle xenoliths. Minerals from harzburgitic and eclogitic parageneses are absent or extremely rare. Indicator mineral data for the Seed kimber-

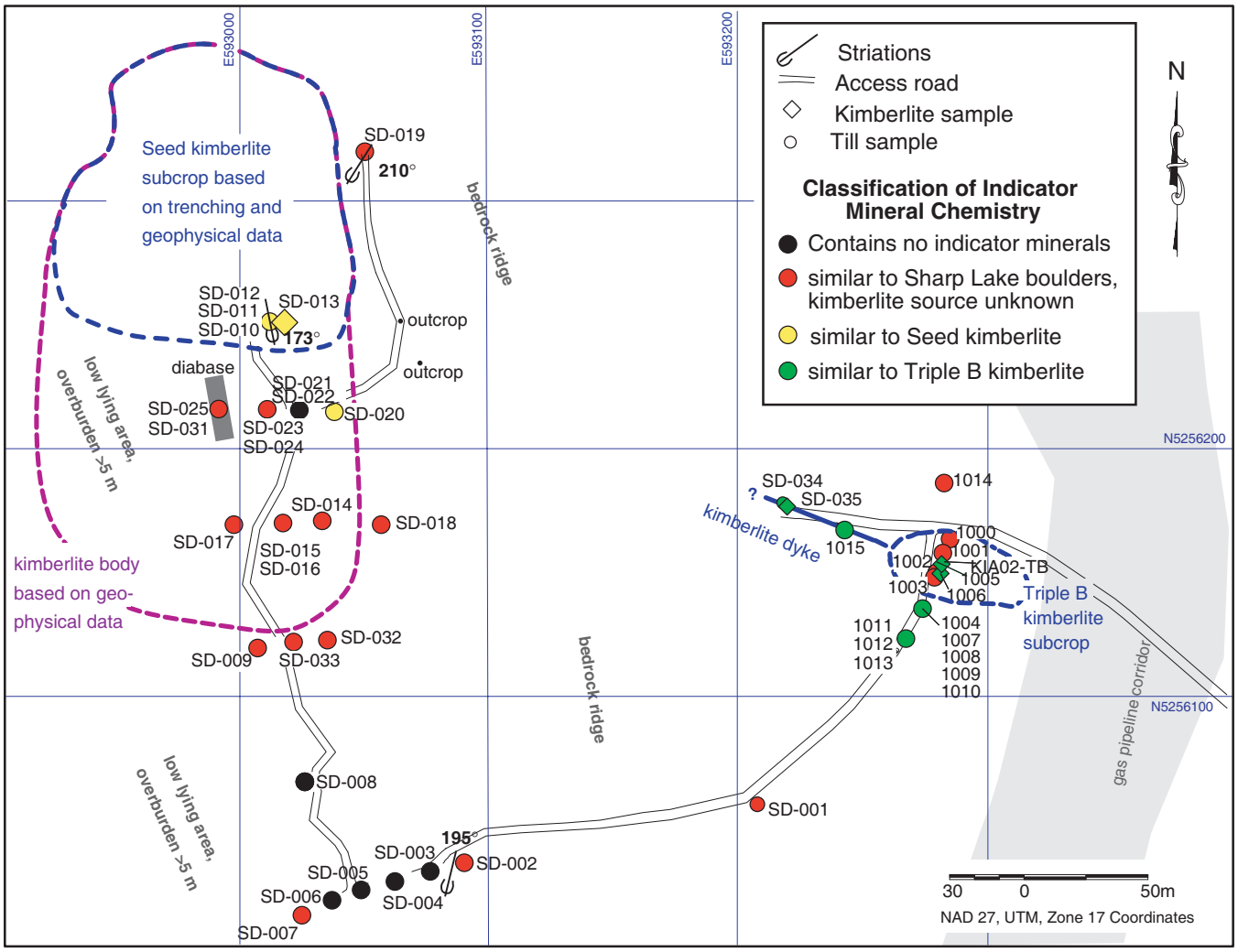

Figure 25. Location of till samples collected around the Seed and Triple B kimberlites and their classification (colour coded), based on mineral chemistry and abundance, as to their kimberlite source.

lite reported here show a significantly wider range of Mg-ilmenite compositions, a more restricted range of garnet compositions, and a lower proportion of chromite grains as compared to data previously published by Sage (2000). These differences in indicator mineral chemistry may be related to differences in the phase of kimberlite sampled. Kimberlite sample MPB-SD-013 used in this study is a volcaniclastic ('diatreme') kimberlite breccia, was sampled from the subcropping kimberlite surface, whereas Sage's (2000) data are based on drill core samples of hypabyssal kimberlite from deeper levels in the Seed kimberlite.

In contrast to kimberlite, till down-ice contains moderate and approximately equal proportions of kimberlitic Mg-ilmenite, crustal ilmenite, and Cr-diopside, whereas chromite and garnet are rare. Only two till samples (MPB-SD-010 and MPB-SD-020) contain Mg-ilmenite and Cr-diopside with the same composition as the kimberlite (Fig. 25). Mg-ilmenite compositions in most till samples down-ice from Seed are characterized by low MgO, very low Cr and show almost no compositional overlap with those from the Seed kimberlite, indicating that they might be derived from a different kimberlite. The compositions are unlike any Mg-ilmenite compositions from known kimberlites in the Lake Timiskaming field but are similar to that reported for GSC till sample TM-MPB-040 (Fig. 13b) (McClenaghan et al., 2001) as well as six kimberlite boulders (Fig. 13c) recovered from gravel deposits exposed in the Sharp Lake esker, 3.5 km southeast of the Seed kimberlite (McClenaghan et al., 2002b; Kjarsgaard et al., 2004).

The high abundance and relative proportion of Cr-diopside and chromite grains in the till south of the Seed kimberlite are inconsistent with those for the Seed kimberlite. The composition of Cr-diopside in most till samples is similar to compositions found in regional till samples in the Kirkland Lake to Marten River region (e.g. McClenaghan et al., 1999, 2001, 2002a). Thus, it is suspected that Cr-diopside-bearing ultramafic rocks in the region are the source of the Cr-diopside, and possibly the chromite and low Mg- ilmenite in the till south of the Seed kimberlite.

The Seed kimberlite contains a few thousand indicator minerals per 10 kg of kimberlite in the 0.25 to 0.5 mm fraction, which is a moderate indicator mineral content as compared to other kimberlites in the Lake Timiskaming field. The abundance of indicator minerals in till south of the Seed kimberlite, however, is low (tens of grains) compared to the

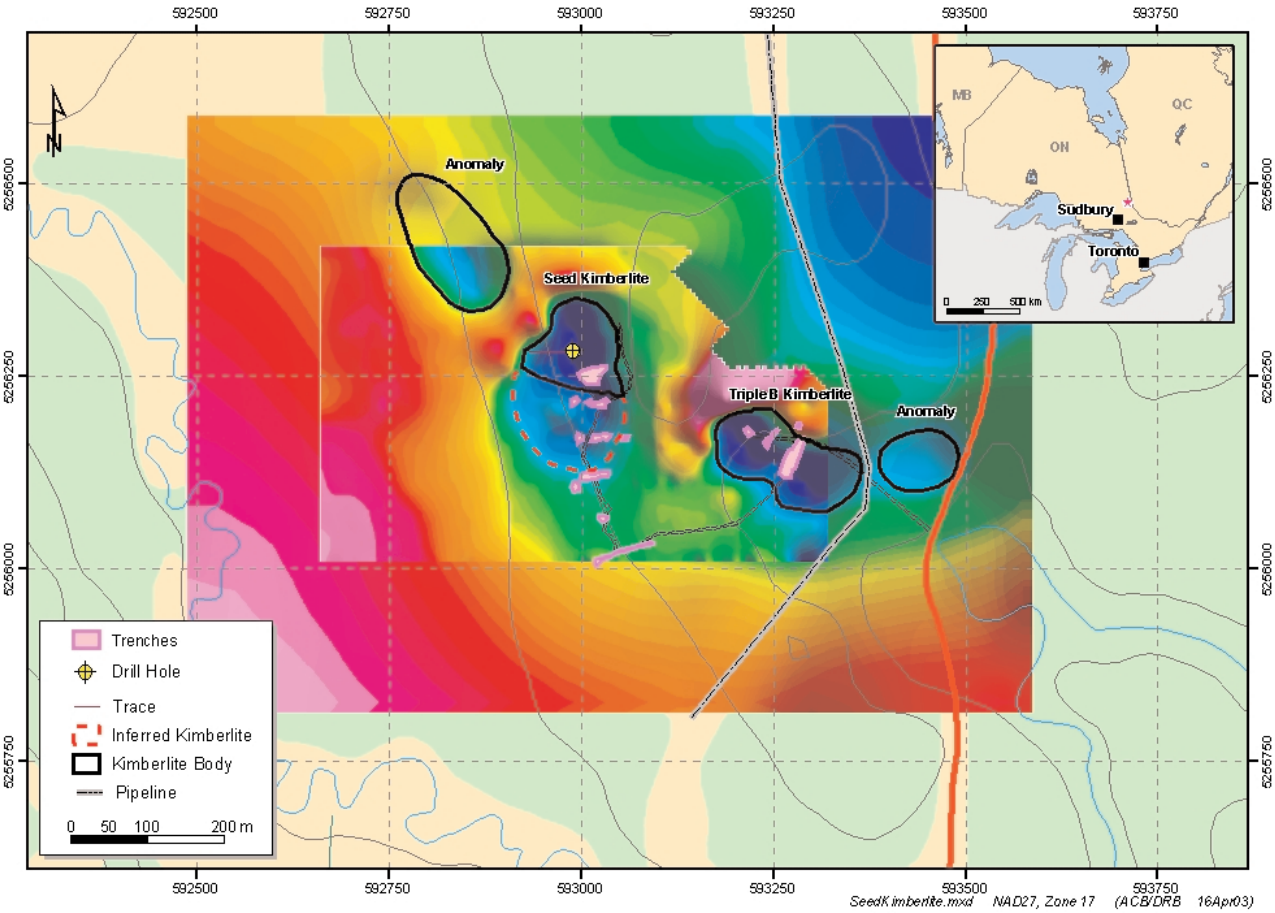

Figure 26. Airborne magnetic survey and ground geophsyical survey (inset) showing the negative magnetic anomalies associated with the Seed and Triple kimberlites, as well as two untested negative magnetic anomalies nearby outlined by thick black lines. Location of GSC trenches indicated in pink (unpublished geophysical data courtesy of De Beers Canada Exploration Inc., 2003).

kimberlite. The few indicator grains in till down-ice combined with the fact that their mineral chemistry indicates they are not derived from the Seed kimberlite indicates that there is not a glacial dispersal train immediately south or southeast of the kimberlite. Possible explanations for the absence of a dispersal train are:

1) the ice flow phase associated with till deposition overlying and down-ice of the Seed kimberlite did not erode and entrain debris from the Seed kimberlite;
2) the overriding glacier eroded and entrained debris from the Seed kimberlite but deposited it either farther south or southwest, beyond the sampled area.

Triple B Kimberlite

The relative abundance of indicator minerals in the Triple B kimberlite is: Mg-ilmenite>>Cr-diopside>pyrope>olivine>chromite. Indicator minerals from the four Triple B kimberlite samples representing three different kimberlite phases have similar chemical compositions. Mg-ilmenite compositions in the three samples from the main Triple B kimberlite body are virtually identical and only the kimberlite dyke shows a more restricted range of Mg-ilmenite compositions, and a greater compositional variation in garnet compositions. In comparison to the Seed kimberlite, the Triple B kimberlite contains higher, although variable amounts of peridotitic and megacryst garnet, peridotitic Cr-diopside, olivine and chromite, indicating that the Triple B kimberlite contained more mantle lherzolite xenoliths as compared to the Seed kimberlite. The Triple B Mg-ilmenite composition is almost identical to that of the Seed kimberlite (Fig. 13a,d).

The Triple B kimberlite contains several thousands of indicator minerals per 10 kg of kimberlite in the 0.25 to 0.5 mm fraction, which is typical of other kimberlites in the Lake Timiskaming field. As expected, till samples up-ice and directly overlying the Triple B kimberlite and dyke are indicator mineral-poor (tens of grains) as compared to samples collected down-ice from the kimberlite. Till samples down-ice from the kimberlite contain thousands of indicator minerals in approximately the same relative proportion as the kimberlite. Mg-ilmenite grain compositions in these till samples indicate that most are derived from the Triple B kimberlite or dyke (Fig. 25). Indicator-mineral-poor samples MPB-02-1000 to MPB-02-1003, overlying the kimberlite, and sample MPB-SD-001, 100 m southwest of the Triple B kimberlite, contain Mg-ilmenite with compositions similar to those from till samples south of the Seed kimberlite (Fig.

25), till sample TM-MPB-040 and the Sharp Lake kimberlite boulders (Fig. 13). The kimberlite source of these Mg-ilmenite grains in the till samples could be the untested magnetic anomaly just northwest of the Seed kimberlite (Fig. 26) or some other unknown kimberlite north to northwest of the Seed kimberlite.

The distributions of Mg-ilmenite and pyrope in till around the Triple B kimberlite (Fig. 10a,b) are similar. Till samples overlying the kimberlite contain a few tens of grains. Just south of the kimberlite, abundance significantly increases, with the highest concentrations forming a ribbon-shaped pattern of consistent concentrations towards the south in the lower parts of the till unit. These high concentrations south of the kimberlite suggests that most of the Mg-ilmenite and pyrope in the till is derived from the south part of the kimberlite body. Olivine abundance in till (Fig. 10c) displays a different pattern from Mg-ilmenite and pyrope in that concentrations are higher overlying the kimberlite (samples MPB-02-1002 and MPB-02-1003) and concentrations increase to the south to maximum values in the farthest till samples (MPB-02-1013, MPB-02-1011). The pattern suggests that olivine in the till is derived from a different part of the kimberlite than the Mg-ilmenite and pyrope, possibly from the northern end of the kimberlite or from parts not sampled in this study.

Till Geochemistry

Till south of the Triple B kimberlite contains a distinctive "kimberlitic" geochemical signature defined by relatively high concentrations of MgO, MnO, Ni, Ba, Sr, LREE, Ta, Nb, TiO_2, P_2O_5, Cr_2O_3, Sr, Th, U, and Co. This is not unexpected as this till contains abundant kimberlite pebbles, thousands of indicator minerals, and its matrix is green, similar to the altered light green volcaniclastic phase of the Triple B kimberlite. The elevated element concentrations reflect the incorporation of abundant kimberlite debris into till. For example, elevated concentrations of MgO and Ni in till reflect the presence of olivine and its alteration product serpentine. High contents of Cr_2O_3 are due to high abundances of Cr-spinel, Cr-pyrope, and Cr-diopside grains. Elevated values for Nb, Ta, and TiO_2 reflect the presence of groundmass perovskite and ilmenite. Elevated Ba and Rb are due to phlogopite, high levels of P_2O_5 and LREE are caused by apatite (and perovskite for REE), and elevated Sr may be due to carbonate minerals and apatite.

For till near surface south of the kimberlite, the <0.063 mm (clay-sized) fraction contains the lowest concentrations of kimberlite pathfinder elements. For till near the bedrock interface, the <0.063 mm as well as the 0.63 to 0.25 mm fractions contains the greatest abundances of pathfinder elements. The lowest values in the finest fraction of the till near surface may be related to the effects of postglacial weathering and leaching. Element concentrations are higher in the near surface till samples for most kimberlite pathfinder elements, except for MgO and Ni, as compared to till samples near the bedrock interface. This pattern may also be related to the effects of postglacial surface weathering.

Comparison of till geochemistry with indicator mineral and pebble counts (Fig. 24) indicates that a kimberlitic geochemical response is detectable in till matrix in samples that contain hundreds of indicator minerals per 10 kg and >7% kimberlite pebbles. For the Triple B kimberlite, geochemical responses were detected when till samples contained more than 300 Mg-ilmenite, 100 Cr-pyrope, and 92 Cr-diopside grains. Identification of a strong kimberlite geochemical signature in till has significant implications for drift prospecting. Till geochemistry is a rapid and inexpensive method (~$35 per sample) that can be used to prescreen bulk till samples collected for indicator mineral analysis. Those till samples that have a strong kimberlitic geochemical response, similar to that defined here and for other kimberlites (e.g. McClenaghan et al., 1999, 2002a) are more likely to contain a significant number of indicator minerals. Potentially indicator-mineral-rich samples can be assigned a higher priority for heavy mineral processing and/or indicator mineral analysis, a costly and time-consuming technique.

CONCLUSIONS

The Triple B kimberlite consists of several different phases: hypabyssal kimberlite, dark green volcaniclastic (diatreme') kimberlite, and its highly altered light green, equivalent. Mg-ilmenite compositions in all three phases are almost identical to each other and to the Seed kimberlite. Some of the variations in relative proportions of indicator minerals (pyrope, Cr-diopside, chromite) in the different kimberlite samples are ascribed to differences in mantle xenolith content. Both kimberlites contain 1000s of indicator minerals in a 10 kg sample, the Seed kimberlite is dominated by Mg-ilmenite and the Triple B kimberlite is dominated by Mg-ilmenite, Cr-diopside, and pyrope.

The Seed and Triple B kimberlite are 240 m apart with a dyke extending northwest from the Triple B kimberlite towards the Seed pipe. Although the dyke was not traced further northwest at the surface, the two kimberlites may be linked by this dyke. Both kimberlites display strong negative magnetic responses and are associated with two similar untested magnetic lows just northwest and east, which also are likely kimberlites.

The indicator mineral chemistry of Mg-ilmenite in till down-ice from the Seed kimberlite and up-ice from the Triple B kimberlite is compositionally different from Mg-ilmenite in the two kimberlites, implying these grains are derived from another kimberlite source(s). The Mg-ilmenite signature is similar to that from till sample TM-MPB-040 (McClenaghan et al., 2001) 9 km south of the Seed and Triple B kimberlites (Fig. 1), as well from six kimberlite boulders found in the Sharp Lake gravel pit 5 km to the southeast (McClenaghan et al., 2002b; Kjarsgaard et al., 2004). It is speculated that the kimberlite source of the Mg-ilmenite grains in till and the boulders around the Seed kimberlite may be the untested magnetic anomalies just northwest of the Seed kimberlite or east of the Triple B kimberlite (Fig. 24).

Down-ice of the Triple B kimberlite, till is composed almost exclusively of kimberlite debris as indicated by its green-yellow colour, the presence of abundant kimberlite clasts, the presence of thousands of kimberlite indicator minerals, and the strong increase in kimberlite specific elements in the till matrix. Kimberlitic debris has been dispersed for at least 20 m down-ice, the limit of this study, but likely

extends further. Kimberlite pathfinder elements include MgO, Ni, Ba, LREE, Ta, Nb, TiO_2, P_2O_5, Cr_2O_3, Sr, Th, U, and CaO and they are most enriched in the <0.063 mm (silt + clay) and the 0.063 to 0.25 mm (fine sand) fractions near the bedrock interface and in the 0.063 to 0.25 mm (fine sand) and 0.25 to 0.50 mm (medium sand) fractions in shallow till near surface. Enrichment factors for these elements are up to 30 times (e.g. Nb and Ta) compared to background till samples up-ice (north).

A kimberlitic geochemical response is detectable in the matrix fraction of till samples that contain a minimum of hundreds of indicator minerals per 10 kg and at least 7% kimberlite pebbles. The relationship between indicator mineral abundance and geochemical response has significant implications for the use of till geochemistry to kimberlite exploration in glaciated terrain because till geochemistry can be used to prescreen bulk till samples collected for indicator mineral analysis. Samples that have a kimberlitic geochemical signature can be assigned a higher priority for heavy mineral processing and indicator mineral analysis. Also noteworthy is the fact that the highest concentrations of kimberlite pebbles, indicator minerals, and pathfinder elements in till are to the south of the kimberlite, not overlying it.

The kimberlite glacial dispersal studies described here for two kimberlites represent end members of a spectrum of kimberlitic signatures in till. The Triple B kimberlite displays excellent examples of very strong mineralogical, pebble lithological, and matrix geochemical signatures in till down-ice of the kimberlite. The subcropping surface of the kimberlite is deeply (>6 m) weathered. In contrast the Seed kimberlite, 240 m to the west, is an example of a kimberlite that is virtually undetectable using till heavy mineral techniques. The subcropping surface of this kimberlite consists of fresh, striated kimberlite. Both situations may be encountered when exploring for kimberlites in the Lake Timiskaming region and other kimberlites fields elsewhere in glaciated terrain.

ACKNOWLEDGEMENTS

This study was funded by the Geological Survey of Canada under the Targeted Geoscience Initiative (TGI), Project 000022 between 2000 and 2003. Mr. Jeff Seed is thanked for allowing access to his property. Mr. D. Boucher of De Beers Canada Exploration Inc. is thanked for providing unpublished geophysical data for the Seed-Triple B area. Excellent service was provided by: Polk Geological Services (ground magnetic and topographic surveys); Overburden Drilling Management Ltd. (sample processing); I.&M. Morrison Geological Services (indicator mineral picking); and Lakefield Research Ltd. (grain mounting and polishing). Comments by R.A. Klassen (GSC) improved the manuscript.

REFERENCES

Burgers, K.M., Boucher, D., and Kong, J.
1998: The petrography of the OPAP kimberlites, New Liskeard area, Ontario, Canada; Extended Abstracts, 7th International Kimberlite Conference, Cape Town (unpaginated addendum).

Fipke, C.E., Gurney, J.J., and Moore, R.O.
1995: Diamond Exploration Techniques Emphasizing Indicator Mineral Geochemistry and Canadian Examples; Geological Survey of Canada, Bulletin 423, 86 p.

Govindaraju, K.
1994: Compilation of working values and sample descriptions for 383 geostandards; Geostandards Newsletter, v. XVIII, Appendix 1, p. 4.

Gurney, J.J.
1984: A correlation between garnets and diamonds in kimberlites; In: Kimberlite Occurrence and Origin: A basis for conceptual models in exploration; Geology Department and University Extension, University of Western Australia, Publication No. 8, p. 143-166.

Heaman, L.M. and Kjarsgaard, B.A.
2000: Timing of eastern North American kimberlite magmatism: Continental extension of the Great Meteor hotspot track; Earth and Planetary Science Letters v. 178, p. 253-268.

Johns, G.W. and Van Steenburgh, R.
1984: Firstbrook and parts of surrounding townships; Ontario Geological Survey Map 2474, Precambrian Geology Series, scale 1" to 1/2 mile.

Kjarsgaard, B.A., McClenaghan, M.B., Boucher, D.F., and Kivi, K.
2003. Kimberlites and ultrabasic rocks of the Wawa, Chapleau, Kirkland Lake and Lake Timiskaming area; in Northern Ontario Field Trip Guide Book, VIIIth International Kimberlite Conference, p. 1-38.

Kjarsgaard, I.M., McClenaghan, M.B., Kjarsgaard, B.A., and Heaman, L.M.
2004: Mineralogy of kimberlite boulders from eskers in the Kirkland Lake and Lake Timiskaming areas, northeastern Ontario, Canada. Lithos.

Kopylova, M.G., Russell, J.K., and Cookenboo, H.
1999: Petrology of peridotite and pyroxenite xenoliths from the Jericho kimberlite: implications for the thermal state of the mantle beneath the Slave Craton, Northern Canada; Journal of petrology, v. 40, p. 79-104.

Lightfoot, P.C., De Souza, H., and Doherty, W.
1993: Differentiation and source of the Nipissing Diabase intrusions, Ontario, Canada; Canadian Journal of Earth Sciences, v. 30, p. 1123- 1140.

Mitchell, R.H.
1986: Kimberlites: Mineralogy, Geochemistry, and Petrology; Plenum Publishing Corporation, New York, 442 p.
1995: Kimberlites, Orangeites and Related Rocks; Plenum Press, New York, 410 p.

McClenaghan, M.B. and Kjarsgaard, B.A.
2003: The Seed and Triple B kimberlites and associated glacial sediments, Lake Timiskaming, Ontario; Geological Survey of Canada, Open File 4492, 1 CD-ROM.

McClenaghan, M.B. and Veillette, J.J.
2001: Surficial geology: Ice flow indicators for the New Liskeard-Temagami area; Geological Survey of Canada, Open File 3385, scale 1:100 000.

McClenaghan, M.B., Kjarsgaard B.A., Kjarsgaard I.M., and Paulen, R.C.
1999: Mineralogy and Geochemistry of the Peddie Kimberlite and Associated Glacial Sediments, Lake Timiskaming, Ontario; Geological Survey of Canada, Open File 3775, 190 p.

McClenaghan, M.B., Kjarsgaard, I.M., and Kjarsgaard, B.A.
2001: Reconnaissance-scale till survey in the New Liskeard-Temagami region, Ontario: Kimberlite indicator minerals and geochemistry; Geological Survey of Canada, Open File 4086, 91 p.

McClenaghan, M.B., Kjarsgaard, B.A., and Kjarsgaard, I.M.
2002a: Indicator mineral content and geochemistry of till around the Peddie kimberlite, Lake Timiskaming, Ontario; Geological Survey of Canada, Open File 4262, 132 p..

McClenaghan, M.B., Kjarsgaard, I.M. and Kjarsgaard, B.A., and Heaman, L.M.
2002b: Mineralogy of kimberlite boulders from eskers in the Lake Timiskaming and Kirkland Lake areas, northeastern Ontario; Geological Survey of Canada, Open File 4361, scale 1:50 000.

McClenaghan, M.B., Kjarsgaard, I.M., and Kjarsgaard, B.A.
2003: Mineralogy and geochemistry of the McLean kimberlite and associated glacial sediments, Lake Timiskaming, Ontario; Geological Survey of Canada, Open File 1762, 1CD-ROM.

Muggeridge, M.T.
1995: Pathfinder sampling techniques for locating primary sources of diamond; recovery of indicator minerals, diamonds and geochemical signatures; Journal of Geochemical Exploration, v. 53, p.183-204.

Sage, R.P.
1996: Kimberlites of the Lake Timiskaming Structural Zone; Ontario Geological Survey, Open File Report 5937, 435 p.
2000: Kimberlites of the Lake Timiskaming Structural Zone; Supplement; Ontario Geological Survey, Open File Report 5937, 123 p.

Sobolev, N.V.
1977: Deep-seated Inclusions in Kimberlites and the Problem of the Composition of the Upper Mantle; (translated from the Russian edition, 1974), American Geophysical Union, Washington, 279 p.

Veillette, J.J.
1986: Surficial geology, Haileybury, Ontario-Quebec; Geological Survey of Canada, Map 1642A, scale 1:100 000.
1989: Ice movements, till sheets and glacial transport in Abitibi-Timiskaming, Quebec and Ontario; in Drift Prospecting (ed.) R.N.W. DiLabio and W.B. Coker; Geological Survey of Canada, Paper 89-20, p. 139-154.
1996: Géomorphologie et géologie du Quaternaire du Témiscamingue, Québec et Ontario; Geological Survey of Canada, Bulletin 476, 269 p.

Veillette, J.J. and McClenaghan, M.B.
1996: Sequence of ice flow in the Abitibi-Timiskaming region: implications for mineral exploration and dispersal of carbonate rocks from the Hudson Bay Basin, Quebec and Ontario; Geological Survey of Canada, Open File 3033, scale 1:500 000.

Young, G.M. and Nesbitt, H.M.
1999: Paleoclimatology, and provenance of the glaciogenic Gowganda Formation (Paleoproterozoic), Ontario, Canada: a chemostratigraphic approach; Geological Society of America Bulletin, v.111, p.264 - 274.